Graduate Program in Sustainability Science - Global Leadership Initiative
Graduate School of Frontier Sciences
The University of Tokyo

2021
Master's Thesis

A Dynamic Energy Budget Individual-based Model (DEB-IBM) for the Japanese Anchovy *Engraulis japonicus*

Submitted July 21st, 2021

Adviser: Professor Shingo Kimura
Co-adviser: Shogo Kudo

Neil Aaron Waters

A DYNAMIC ENERGY BUDGET INDIVIDUAL-BASED MODEL (DEB-IBM) FOR THE JAPANESE ANCHOVY ENGRAULIS JAPONICUS

Acknowledgements

First and foremost, I must thank Akinori Takasuka and Michio Yoneda, whose generosity and kindness made this study possible. I would also like to thank my supervisor, Shingo Kimura, for giving me total freedom to pursue my interests.

The continued assistance and patience of the Dynamic Energy Budget research community has been invaluable, in particular the help of Nina Marn, Marko Jusup, Dina Lika and Bas Kooijman. A special thank-you to Dylan Waters, Nana Miyakawa and Lili Garcia; their creativity and intelligence guided the way more than once.

Lastly, I am deeply grateful for the financial assistance of the Tonen International Scholarship Foundation. It is little exaggeration to say their support was a life-saver.

Table of Contents

1 Introduction

1.1 The Warming Ocean

Earth is facing a climate emergency (Lenton *et al.* 2019). One result is ocean warming: average temperature, temperature variability and the frequency of extreme temperature events (e.g. heat waves) are projected to increase over the coming decades (IPCC 2019). More than other environmental factors such as salinity or biotic competition, water temperature is the single most important driver of fishery species' geographical ranges, individual physiological rates and population growth rates (Branders *et al.* 2015; Enders *et al.* 2016; Sunday *et al.* 2012).

As a result of warming, changes to spatial and temporal distribution, abundance, size and other life history traits are expected for many fishery species, for example the observed poleward migrations of many marine species (Cheung *et al.* 2009; Brander *et al.* 2015). Such changes impact the sustainability of fisheries and marine ecosystems (Sumaila *et al.* 2011; Barange *et al.* 2018). To mitigate losses we must anticipate how key fish species will respond to a warming ocean.

1.2 Modelling the Japanese Anchovy

The Japanese anchovy *Engraulis japonicus* is an abundant and widely distributed species in the north-western Pacific Ocean (Whitehead *et al.* 1988). As a small plankton-feeding pelagic fish, *E. japonicus* acts as a keystone species linking trophic levels of the marine food web (Cury *et al.* 2000). It has been of great commercial importance in Japan for the past century, and in China in recent decades (Hayasi 1966; Zhao *et al.* 2003). A typical feature of small pelagic fish like *E. japonicus* is their tight link to environmental conditions, which has profound effects on their population dynamics (Bueno-Pardo *et al.* 2020; Checkley *et al.* 2009). The goal of this study is to determine how the ecologically and economically important *E. japonicus* will be affected by ocean warming expected under climate change.

Up until now there has already been great research interest in using models to understand the mechanisms underlying *E japonicus*' dramatic responses to even subtle shifts in environmental conditions (Chavez *et al.* 2003; Takasuka *et al.* 2007). Research up until now can be separated into two main avenues of modelling: empirical and process-based.

1.2.1 *E. japonicus* and Empirical Models

A common type of empirical model makes predictions of species' response based on observed correlations between environmental variables and historical records of species' response (Robertson *et al.* 2003). These 'correlative models' are widely-used, time-efficient tools that can reveal the presence of hitherto unknown drivers of response to environmental change. Such empirical models have provided valuable insight into the relationship between environmental conditions and the dynamics of *E. japonicus*.

Zhou *et al.* (2015) clarified the link between the Pacific decadal oscillation and patterns of anchovy abundance; Kuwae *et al.* (2017) revealed the famous alternating boom-bust cycle shared between anchovy and sardine to be a relatively recent phenomenon of the 20th century. Empirical models have revealed how hydrodynamic processes affect egg and larval

transport (Takeshige *et al.* 2015) and have predicted northward migration and increases in abundance for anchovy under climate change (Liu *et al.* 2020). These predictions can be illuminating but are also limited because empirical models cannot identify the mechanisms that drive observations.

For instance, Yu *et al.* (2020) found recruitment to be negatively correlated with sea surface temperatures (SST) in July and positively correlated with surface-level zooplankton biomass. This suggests both temperature and food are important, and that a warming ocean will have both direct (temperature) and indirect (altered currents changing zooplankton abundance) effects on anchovy recruitment. What remains unclear, however, is which aspect of anchovy biology drives these findings. Indeed, another empirical study using convergent cross mapping, a non-correlative technique, was able to ascertain the importance of temperature in anchovy recruitment but could not comment on which aspect of physiology was responsible (Nakayama *et al.* 2018).

While empirical models are certainly valuable tools, since they do not indicate the direction of relationships, presence of covarying factors, or mechanisms driving observations, they are not always the appropriate choice. This is particularly true for predictions of how species will respond to climate change; whether the statistical relationships that infer correlations will remain robust under increasingly variable environments is uncertain. For such problems, process-based models may be more appropriate.

1.2.2 *E. japonicus* and Process-based Models

Often referred to as ‘mechanistic’ or ‘bioenergetic’ models, process-based models attempt to simulate the mechanisms that underlie the correlations between environmental variables and a species’ life history, distribution or abundance (Robertson *et al.* 2003). The more direct link between environment and physiology allows them to outperform correlative models in predicting biological responses to environmental change when used in the appropriate context (Naman *et al.* 2019).

While such models are rarely perfect, even flawed output can be a valuable source of information pertaining to a species’ life history traits. The issue with process-based models is that they are relatively laborious and require a wealth of detailed physiological data to parameterise (Wang *et al.* 2013). When such data is not available, costly laboratory experiments are needed. This often limits the application of process-based models to species that have been well studied (Nisbet *et al.* 2012).

Fortunately, *E. japonicus* is a relatively well-studied species. Process-based models have been used to elucidate growth, in-situ food conditions and the minimum levels of food required for reproductive success (Zenitani and Kono 2013). Simulations have also been used to elucidate drivers of migrations; those in winter are presumably driven by temperature and migrations prior to spawning are likely for better access to food (Wang *et al.* 2013).

Even for the well-studied *E. japonicus*, however, process-based models have not been able to fully clarify the

mechanisms by which individuals respond to environmental conditions. Zenitani *et al*. (2009) found growth rate to be more dependent on food (copepod) availability than temperature, whereas Takasuka & Aoki (2006) found temperature to be most important. This supports the idea that physiological responses of *E. japonicus* to environmental conditions vary across regions (Takasuka & Aoki 2006). Unfortunately, process-based models are usually tailored to a single species, or region-specific population or life stage of that species, from which the parameters of the model were derived (Urtizberea *et al.* 2008). Furthermore, each process-based model is built with its own unique set of assumptions. These factors make comparison of results from different models difficult; in the case of *E. japonicus*, it is difficult to determine if the observed differences in response are due to differences in experienced environmental conditions, epigenetic traits or study methodology.

1.2.3 Summary

To summarise, process-based models and empirical models have been used to reveal many aspects of *E. japonicus* ecology and have served as great tools for marine conversation and fisheries management. Process-based models can adequately describe physiological rates and extrapolate response, but their parameters are numerous and often specific to a single species, life stage or region. Empirical models implicitly include all aspects of species' biology, such as biotic interactions or endogenous factors, but they do not specify mechanisms and their use is limited when extrapolating to unknown or increasingly extreme conditions like climate change.

A more theoretical approach, the Dynamic Energy Budget (DEB) theory, addresses the above problems. It is a general theory based on well-defined assumptions that can be applied to individuals of any species in a consistent manner.

1.3 Advantages of DEB to Model the Impact of Ocean Warming on *E. japonicus*

DEB theory has been successfully used to quantify the effects of varying food and temperature on growth and reproduction for a wide diversity of taxa (Kooijman 2020). Below are outlined a few properties of the DEB model that make it suitable for modelling the impacts of climate change on *E. japonicus*.

Traditional process-based models typically use measurable rates to define the state of an individual, *e.g.* respiration rate. However, the way such rates are measured and defined differ slightly between studies (Nisbet *et al.* 2012) or are often modelled incorrectly (Kooijman 2020), impeding holistic understanding. Perhaps the greatest advantage of DEB is its generality; the theory aims to find the common physical properties of metabolic organisation across all life (Kooijman 2010). The Add-my-Pet (AmP) database contains parameter values and the data from which they are derived for over 1000 animal species. As all species have the same parameters in DEB, the AmP database facilitates easy comparison to understand why species differ in their responses to environmental conditions (Marques *et al.* 2018). As an example, this aspect of AmP could be used to examine the physiological reasons for differing responses to thermal change among the world's anchovies and compare their outlooks under climate change.

Unlike empirical models, the parameters in DEB link environmental forcing to a species' energy budget and

thereby specify which mechanisms are responsible for changes to species' distribution or life history. For instance, in the North Sea, a DEB model was able to clarify that temperature was the mechanism underlying the northward expansion of European anchovy *Engraulis encrasicolus* (Raab *et al.* 2013). The link between environmental conditions and the energy budget is useful for modelling reproduction dynamics as well. Process-based models have traditionally struggled to simulate the fecundity of indeterminate multiple-batch spawners like *E. japonicus* (Pecquerie *et al.* 2009). DEB defines the energy available for spawning throughout the spawning season as a function of the environmental conditions, allowing simulations of spawning frequency and fecundity for species which vary greatly in their reproductive output (Pecquerie *et al.* 2009).

Whereas process-based models have successfully described the effects of environmental conditions on aspects of life history such as recruitment (Zenitani & Kono 2013), such models are often life-stage dependent. DEB mechanistically describes energy flows throughout the entire life cycle. This is important because stressors experienced during the early life stages can impact performance later in life (Monaco *et al.* 2014). The conditions larvae experience and the energy available to them upon hatching are also dependent on the conditions experienced by the adults that preceded them. Since the DEB model encompasses the full lifecycle, the conditions experienced by adults can be directly traced to the conditions and recruitment success experienced by the next generation of larvae (Pecquerie *et al.* 2009).

1.4 From Individual to Population Level: Linking DEB with Individual-based Modelling

In an individual-based model (IBM) a group of unique individuals (sometimes called "agents"), defined by their state variables and how these are affected by the environment, are tracked over full life cycles; thereby facilitating an understanding of population dynamics (Grimm *et al.* 2010).

IBMs link nicely with DEB models. Both use the individual as the fundamental unit from which patterns at larger scales of biological organisation emerge. DEB specifies how environmental conditions affect individual state variables, and thus life-history traits such as growth and reproduction; factors which strongly influence population trends (Martin *et al.* 2012). This is ultimately the information of interest for this study – how will the population of *E. japonicus* as a whole be affected by future temperature conditions?

1.5 The Aims of this Study

This study aims to parameterise a DEB model for *E. japonicus* and construct a DEB-IBM to explore how *E. japonicus* may respond to moderate levels of climate change by the year 2100. The study has 4 objectives:

1) Obtain values of the DEB parameters for *E. japonicus* and explore what these values indicate about *E. japonicus* physiology.
2) Validate the DEB model by reproducing observed life history traits for *E. japonicus*, including season-specific patterns of larval growth.
3) Connect the DEB model with an IBM to create a DEB-IBM that specifies the change in the state variables of many individuals over time, revealing population trends.
4) Assess how physiological traits at the individual level and population dynamics may change due to ocean

warming by the year 2100.

In the following section, the environmental forcing used to simulate climate change until 2100 is explained. The standard DEB model is then described, followed by the parameter estimation process. Implementation of the IBM component of the DEB-IBM follows.

2 Methods

2.1 Environmental Forcing: Obtaining Predictions of Water Temperature until 2100

This model aims to predict the effect of ocean warming, caused by climate change, on the life-history traits and population trends of *E. japonicus*. To do so, predictions of sea temperature were obtained from the World Climate Research Program's Coupled Model Intercomparison Project 6 (CMIP6); specifically the model output from FIO-ESM-2-0's "ssp245" experiment, which stands for Shared Socioeconomic Pathway 2, a scenario representing 'middle of the road' levels of climate change with low or moderate progress on climate change mitigation (Bao *et al.* 2020).

Average monthly potential sea temperature data from 2015 to 2100 were obtained at depths of 5, 25, 55 and 105 metres from 113°E - 140°E, 21.25°N - 48°N, which approximates most of the range and depths commonly experienced by *Engraulis japonicus* (Whitehead *et al*. 1988). Model output was at 1.1° longitudinal resolution and 0.27-0.57° latitudinal resolution. The mean temperature was taken across the 4 depths, and then the monthly mean temperature of the geographical area was calculated. Data manipulation was performed using Climate Data Operators Version 1.9.8 (Schulzweida 2019).

2.2 The DEB Model

Dynamic Energy Budget theory follows the metabolic dynamics of an individual throughout the entire life cycle and specifies how the individual's physiological rates are tied to dynamic temperature and food availability.

2.2.1 The Basic Assumptions of a DEB Model

The standard DEB model quantifies assimilation, growth, maintenance, maturation and reproduction through all stages of a species' lifecycle, from a non-feeding embryo to a reproducing adult (Sousa *et al.* 2010). This is possible because DEB assumes that all organisms operate on the same universal rules of metabolism throughout ontogeny; these rules in turn adhere to the conservation of mass, isotopes, energy and time (Kooijman 2010, Jusup *et al.* 2017). While DEB can describe plants and other life forms, the standard DEB model described here applies to animals only.

DEB aims to be as simple as possible; accordingly the biomass of an individual is described as two aggregated chemical compounds (i.e. two 'pools' of metabolites) that are constant in their chemical composition but vary in their relative amounts; food is also considered of constant chemical composition and at constant food supply the ratio of the two chemical pools does not change (Jusup *et al.* 2017). Despite the simplicity of such assumptions DEB sufficiently reproduces metabolic patterns from the cellular to the population level (Sousa *et al.* 2010, Jusup *et al.* 2017). DEB's aim of quantifying physiological development based on energy and mass conservation rules have allowed it to simultaneously capture patterns produced by numerous empirical models (Kooijman 2020).

2.2.2 The Basic Flow of Energy in a DEB Model

The main metabolic processes of the DEB model, described in the notation for energy (J), are presented in Figure 1, the dynamic equations of the model in Table 1 and the DEB parameters in Table 2.

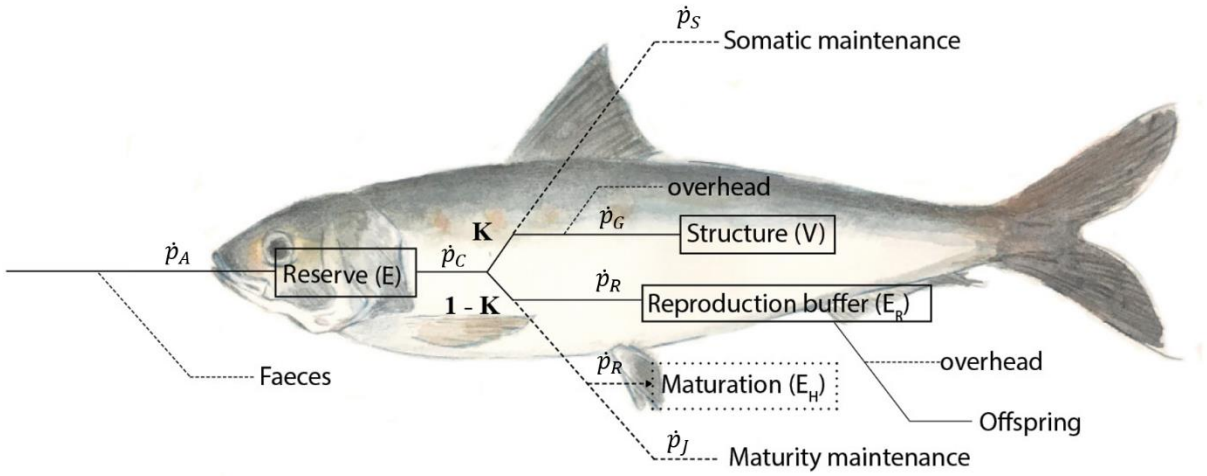

Figure 1. The state variables and main fluxes of the DEB model. State variables are designated with boxes. Fluxes (Joules per day; $J \cdot d^{-1}$) represent energy flows to and from the state variables. $\dot{p}_A$ is the assimilation rate, $\dot{p}_C$ the mobilisation rate, $\dot{p}_G$ the growth rate, $\dot{p}_S$ the somatic maintenance rate, $\dot{p}_J$ the maturity maintenance rate and $\dot{p}_R$ the maturation rate, which becomes the reproduction rate after puberty.

Table 1. The state variables, fluxes and dynamics of the DEB model.

Symbol	Definition
State Variables	
$\boldsymbol{E}$	Reserve
$\boldsymbol{V}$	Structural Volume
$[\boldsymbol{E}]$	Reserve Density: E/V
$\boldsymbol{L}$	Structural Length
$\boldsymbol{E_H}$	Maturity Level
$\boldsymbol{E_R}$	Reproduction Buffer
Fluxes	
$\dot{\boldsymbol{p}}_{\boldsymbol{A}}$	Assimilation rate: $\mathcal{M}\{\dot{p}_{AM}\} f L^2$
$\dot{\boldsymbol{p}}_{\boldsymbol{C}}$	Mobilisation Rate: $E\,\frac{\mathcal{M}\dot{v}[E_G]L^2+\dot{p}_S}{\kappa E+[E_G]L^3}$
$\dot{\boldsymbol{p}}_{\boldsymbol{S}}$	Somatic Maintenance Rate: $[\dot{p_M}]L^3$
$\dot{\boldsymbol{p}}_{\boldsymbol{G}}$	Growth: $\kappa\dot{p}_C - \dot{p}_S$
$\dot{\boldsymbol{p}}_{\boldsymbol{J}}$	Maturity Maintenance Rate: $\dot{k}_J E_H$
$\dot{\boldsymbol{p}}_{\boldsymbol{R}}$	Maturity/Reproduction Rate: $(1-\kappa)\dot{p}_C - \dot{p}_J$
Dynamics of State Variables	
$\frac{\boldsymbol{dE}}{\boldsymbol{dt}} = \dot{\boldsymbol{p}}_{\boldsymbol{A}} - \dot{\boldsymbol{p}}_{\boldsymbol{C}}$	
$\frac{\boldsymbol{dL}}{\boldsymbol{dt}} = \frac{\boldsymbol{1}}{\boldsymbol{3L^2}} - \frac{\dot{\boldsymbol{p}}_{\boldsymbol{G}}}{[\boldsymbol{E_G}]}$	
$\frac{\boldsymbol{dE_H}}{\boldsymbol{dt}} = \dot{\boldsymbol{p}}_{\boldsymbol{R}}\ (\boldsymbol{E_H} < \boldsymbol{E_H^p})$	
$\frac{\boldsymbol{dE_R}}{\boldsymbol{dt}} = \dot{\boldsymbol{p}}_{\boldsymbol{R}}\ (\boldsymbol{E_H} \geq \boldsymbol{E_H^p})$	

Table 2. DEB Parameters. Square brackets [ ] signify a parameter is per unit of structural volume, curly brackets { } signify a parameter is per unit of structural surface area.

Symbol	Units	Definition
Core Parameters		
κ_X	-	Assimilation Efficiency
$\{\dot{p}_{AM}\}$	$J\ cm^{-2}\ d^{-1}$	Surface Area-specific Maximum Assimilation Rate
$\dot{v}$	$cm^{-1}\ d$	Energy Conductance
κ	-	Fraction of Energy Allocated to the Soma
κ_R	-	Reproduction Efficiency
$[\dot{p}_M]$	$J\ cm^{-3}\ d^{-1}$	Volume-specific Somatic Maintenance Rate
$\dot{k}_J$	d^{-1}	Specific Maturity Maintenance Rate Coefficient
$[\mathrm{E}_G]$	$J\ cm^{-3}$	Volume-specific Cost of Structure
E_H^b	J	Birth Threshold
E_H^j	J	Metamorphosis Threshold
E_H^p	J	Puberty Threshold
Auxiliary Parameters		
δ_M	-	Shape Coefficient
$\mathcal{M}$	-	Shape Correction Function; 1 ($E_H^b < \boldsymbol{E_H}$), $\frac{L}{L_b}$ ($E_H^b < \boldsymbol{E_H} < E_H^j$)
$s_{\mathcal{M}}$	-	Maximum Value of Shape Correction Function; $\frac{L_j}{L_b}$ ($E_H^j < \boldsymbol{E_H}$)
T_A	K	Arrhenius Temperature
Other Parameters		
z	-	Zoom factor; $L_m / L_m^{\mathrm{ref}}, L_m^{\mathrm{ref}} = 1cm$
f	-	Scaled functional response
$[\mathrm{E}_M]$	$J\ cm^{-3}$	Maximum Reserve Density; $\{\dot{p}_{AM}\}$ / $\dot{v}$
$\dot{k}_M$	d^{-1}	Somatic Maintenance Rate Coefficient; $[\dot{p}_M]$ / $[\mathrm{E}_G]$
g	-	Energy Investment Ratio; $\frac{[\mathrm{E}_G]}{\kappa[\mathrm{E}_M]}$
κ_G	-	Growth Efficiency
L_m	cm	Maximum Structural Length; $\frac{\kappa\{\dot{p}_{AM}\}}{[\dot{p}_M]}$
L_∞	cm	Ultimate Structural Length; $f\frac{\kappa\{\dot{p}_{AM}\}}{[\dot{p}_M]}\ or\ L_m s_{\mathcal{M}}$

The standard DEB model assumes one type of food, one structure and one reserve. An individual is described by the energy of the state variables: reserve E, structure V, maturity level E_H and reproduction buffer E_R. Energy in the form of food is assimilated from the environment into the reserve. A fixed portion of energy mobilised from the reserve, κ, is used for growth of the structure (i.e. body mass) and somatic maintenance. Somatic maintenance includes maintenance processes such as protein turnover as well as movement. Assimilation is assumed to scale with surface area, whereas structural maintenance is assumed to scale with volume. The other fraction of energy mobilised from the reserve, $1-\kappa$, is used for

maturation and maturity maintenance. Maturity maintenance represents processes that maintain the current level of maturity, e.g. hormone regulation. Somatic maintenance and maturity maintenance costs are paid before growth and maturation, respectively.

Food uptake follows a scaled functional response relationship with food density, where f represents the feeding rate of an individual as a fraction of the maximum feeding rate ($0 < f < 1$). For example, $f = 1$ indicates ad libitum feeding conditions. Ingested food is assimilated to the reserve at an efficiency equal to κ_X.

2.2.3 Maturation and Life Stages

Energy invested in maturity represents an increase in complexity of the organism and does not contribute to mass. Individuals begin life as an embryo, which consists entirely of reserve and does not feed ($\dot{p}_A = 0$). As the reserve is mobilised, transitions to subsequent life stages occur when the energy accumulated in maturity E_H reaches certain thresholds (see table 2). An embryo becomes a larva at the birth threshold E_H^b, a larva becomes a juvenile at the metamorphosis threshold E_H^j and a juvenile becomes an adult at the puberty threshold E_H^p. In DEB, birth represents the start of exogenous feeding, metamorphosis represents the end of accelerated growth and puberty indicates sexual maturity.

2.2.4 Metabolic Acceleration: the 'abj' type DEB Model

The DEB model used in this study is not the standard DEB model, but a one parameter extension thereof called the 'abj' model. The acronym 'abj' stands for acceleration between birth and metamorphosis. The metabolic rate of some species of fish, including anchovy, accelerates during the larval stage to compensate for a retarded metabolic rate during the embryonic stage (Kooijman 2014b, Pecquerie *et al.* 2009). To capture this acceleration, the surface area-dependent parameters $\{\dot{p}_{AM}\}$ and $\dot{v}$ are multiplied by a shape correction function $\mathcal{M}(L)$, which increases linearly with structural length throughout the larval stage in accordance with: $\mathcal{M}(L) = \frac{L}{L_b}$, where L_b is the structural length at mouth opening. This allows for assimilation and reserve mobilisation, normally proportional to surface area, to increase proportionally with volume, thus allowing exponential growth during the larval stage. Upon the completion of metamorphosis ($E_H = E_H^j$), the value of $\mathcal{M}$ is fixed at its maximum value $s_{\mathcal{M}}$, but continues to be applied to the rates of assimilation and mobilisation. This is because metabolic acceleration is permanent. This implies that if two identical individuals undergo metabolic acceleration at different food levels, the individual at higher food level will accelerate to a greater extent; and even after acceleration will permanently have greater metabolic rates (e.g. growth, reproductive rate, maintenance costs; Kooijman *et al.* 2011, Kooijman 2014b).

2.2.5 Reproduction

Allocation of energy switches from maturation to reproduction at puberty, $E_H = E_H^p$. Energy is accumulated in the reproduction buffer until a spawning event, at which point eggs are released. As eggs are simply 'wrapped' reserve,

relatively little energy ($1 - \kappa_R$) is dissipated in the production of eggs (Kooijman 2010; Kooijman 2014a).

2.2.6 Quantifying the Effect of Temperature on Metabolic Rates

The effect of temperature on metabolic rates is quantified using the Arrhenius equation: $\dot{k}(T) = \dot{k}(T_0) * exp\left\{\frac{T_A}{T_0} - \frac{T_A}{T}\right\}$, where the value of metabolic rate $\dot{k}$ at temperature T is given if the value of metabolic rate $\dot{k}$ is known at temperature T_0 (Kooijman 2010). T_A is the Arrhenius temperature, a species-specific parameter that describes a species' thermal sensitivity.

2.3 DEB Parameter Estimation for *Engraulis japonicus*

The aim of the AmP database is to create a catalogue of peer-reviewed entries containing the values of DEB parameters for all species. To facilitate this, the software "AmPtool" and "DEBtool" are available for parameter estimation (Marques *et al.* 2018).

AmPtool and DEBtool were used with MATLAB R2021a to estimate the DEB parameter values for *Engraulis japonicus*. A variety of zero-variate and univariate data were used to inform the estimation procedure, including: time until birth as a function of temperature (Fukuhara 1983), time-length data (Fukuhara & Takao 1988), length-weight data (Funamoto *et al.* 2004) and reproduction rate as a function of temperature at various food levels (Yoneda *et al.* 2014).

The estimation procedure aims to minimise the difference between values predicted by DEB parameters and real-life observed values using a Nelder-Mead search algorithm (Marques *et al.* 2019). It follows the concept of the covariation method, where DEB parameters can be estimated, even when no empirical data are available, using the assumption that all species simply vary in parameters that are based off the same basic metabolic mechanisms (Lika *et al.* 2011).

The goodness of fit for the predictions of the estimated parameters were assessed by Mean Relative Error (MRE) with a range of [0,∞] and Symmetric Mean Squared Error (SMSE) with a range of [0,1] (Marques *et al.* 2019). The completeness of the real data used for the parameter estimation procedure was gauged according to the guidelines by Lika *et al.* (2011).

2.4 From Individual to Population Level: Creating a DEB-IBM

An individual-based model tracks the collective change in state variables of many individuals over time, which defines trends in populations (Bonabeau 2002). An IBM was integrated with the DEB described previously to create a DEB-IBM, where the state of an individual is determined by the DEB model and the IBM allows population rates to be inferred (Grimm and Railsback 2005). The IBM was written using the software Netlogo version 6.1 (Wilensky 1999). The code and concept is based on the DEB-IBM for the standard DEB model developed by Martin *et al.* (2012).

2.4.1 The Basic Structure of the DEB-IBM

The DEB-IBM contains a group of DEB individuals within a changing environment. The model is non-spatial; the individuals are affected only by the thermal environment and do not interact with each other. Food is assumed to be constant and ad libitum. The model simulates 220 timesteps per day in model time, days being the temporal unit specified in DEB equations. The dynamics of the state variables for embryos must be calculated at much smaller timesteps, but because this model assumes constant food, larvae are born with reserve densities equivalent to their mother, making calculations for the initial reserve density of embryos unnecessary (Kooijman 2010).

The monthly average temperature was updated every 30.5 days model time. For the model validation, the model was run in accordance with the data. Otherwise, models were run from 2015 - 2100 model time. Each timestep consists of checking temperature and calculating the changes to state variables. While individual state variables are updated every timestep, the population is only updated once per day (220 timesteps).

2.4.2 Super Individuals

To simulate the population dynamics of *E. japonicus*, described as one of the most abundant fish in the Northwest Pacific (Zhao *et al.* 2003), the "Super-Individual" method was used (Scheffer *et al.* 1995). In the DEB-IBM each unique individual (deemed a super individual) actually represents a greater number of identical sub-individuals. A parameter is introduced to represent the number of identical individuals represented by each super individual: "worth". Changes to population size through recruitment and mortality are quantified through the change in worth of the model's super individuals.

2.4.3 Inter-individual Variability, Model Initialisation & Stock Assessment

To introduce variability between individuals and prevent synchronised population fluctuations each SI has a parameter called the 'scatter multiplier': a log-normally distributed number with a mean of 1 and standard deviation of 0.05 (Kooijman *et al.* 1989). Certain parameters of each SI are multiplied ($\{\dot{p}_{AM}\}$) or divided (E_H^b, E_H^j, E_H^p, g) by their scatter-multiplier to make each individual unique in their state variables (Martin *et al.* 2012).

The model aims to reproduce the stock dynamics of the Tsushima Warm Current. The number of eggs laid for this region in 2016 was estimated to be 1345 trillion (Yatsu 2019). This number is split across 10 SIs. Following observations that daily egg mortality is very high in *E. japonicus* (Wan & Bian 2012), an estimated daily mortality rate of 0.89 d^{-1} was applied to the model (Kim and Lo 2001). The model is initiated with the proportion of larvae that survive the period of egg mortality. Egg and non-feeding larval dynamics are not calculated explicitly because the timestep size required for accurate estimation of the embryo dynamics is too small for the DEB-IBM. All SIs begin the model with a reserve density equal to 1, which is expected for larvae that hatch under ad libitum food conditions (Kooijman 2010).

The model is initialised on January 1st, 2015 and run until January 1st, 2100. Years 2015 – 2020 are used as a 'spin-

up' period to stabilise the population (Bueno-Pardo *et al.* 2020). The spin-up period is not included in analyses. Stock size is estimated by multiplying the total number of anchovies (i.e. total worth of all SIs) by the mean wet weight of SIs and converting from grams to tonnes. The DEB-IBM population is capped at 100 SIs due to computational limitations.

2.4.4 Reproduction & Mortality

The aim of the reproduction submodule was to recreate a spawning frequency (number of spawning events per day during the spawning season) and relative batch fecundity (RBF; number of eggs per batch per gram of body weight) similar to those observed for *E. japonicus*. RBF was chosen as a reproductive variable following observations that anchovy females are thought to allocate an amount of energy proportional to their body size towards egg production (Imai and Tanaka 1997; Yoneda *et al.* 2015). All SIs in the model are considered female. An SI reproduces if:

i) They are sexually mature ($E_H > E_H^p$)
ii) The water temperature is greater than 15℃ (Funamoto *et al.* 2004)
iii) The energy in the reproductive buffer is greater than the target batch size ($E_R > E_B;\ E_B = RBF \cdot W_w.$)

To determine the target batch size, a value recorded for ad libitum conditions was used: RBF = 572 (Yoneda *et al.* 2013). One new SI is created each spawning event. The worth of the new SI (the number of individuals the SI represents) is equal to the total number of eggs spawned during the last spawning event, subtract the number of eggs expected to die due to natural mortality. In the model individuals will spawn throughout the year if the above conditions are satisfied, following observations that *E. japonicus* spawn year-round in some regions (Takasuka *et al*. 2017).

Estimates of non-embryonic mortality rates were obtained from studies using catch-curve analyses of anchovy samples from commercial fishing nets and ichthyoplankton surveys (Kim and Lo 2001, Jung *et al.* 2008). Mortality rates based on length classes (SL) were implemented: > 2 cm = 0.1589 d^{-1}, 2 – 3.79 cm = 0.0483 d^{-1}, 3.8 – 6.65 cm = 0.0202 d^{-1}, 6.66 – 8.55 cm = 0.0106 d^{-1}, 8.56 – 11.41 cm = 0.0065 d^{-1}, > 11.41 cm = 0.0031 d^{-1} (Jung *et al.* 2008). Each day the mortality rate for each SI is determined and its worth is reduced accordingly. An SI is removed from the model if its worth decreases below 10 or if its age exceeds 36 months.

2.5 DEB-IBM Model Validation

To validate the model, simulations were run to try to replicate *E. japonicus* larval growth data from Sagami Bay (Takasuka *et al.* 2017). Larval growth was chosen as a validity metric because it is difficult to simulate compared to other life stages or rates; growth during this stage is not linear and key life history traits are dependent not only on the external environment but also the timing of mouth-opening and metamorphosis.

Monthly average sea surface temperatures (SST) were obtained for Sagami Bay for the duration of the larval growth study: October 2003 – February 2005. Using these temperatures as environmental forcing input for the model, and assuming a scaled functional response of $f = 1$, simulations were run to see if the model could reproduce the length-at-age and growth rates observed by Takasuka *et al.* (2017).

3 Results

3.1 Results of DEB Parameter Estimation For *E. japonicus*

Table 3 displays the DEB parameter values resulting from the estimation procedure. The completeness of data used for the estimation procedure was deemed 3.0; the maximum 10 signifies data that describes a species' thermal, mass and entropy budget for the full cycle at varying levels of food and temperature (Lika *et al.* 2011). To date the highest score for data completeness on the AmP database is 5.0. The MRE of the estimated DEB values is 0.149, the SMSE 0.169. Both of these values are reasonable for an estimation with data completeness of 3.0 (Marques *et al.* 2018).

Table 3. DEB parameter values estimated for *E. japonicus*, compared with published parameter values of the *E. encrasicolus* and *E. anchoita*.

		E. japonicus		*E. encrasicolus*		*E. anchoita*			
Symbol	**Units**	**Value**	**°C**	**Value**	**°C**	**Value**	**°C**	***f***	**Description**
T_{typ}	°C	18.4	-	15	-	8	-	-	Typical Body Temp.
T_A	K	6071	-	9800	-	9800*	-	-	Arrhenius Temp.
z	-	0.477	-	0.202	-	3.051	-	-	Zoom Factor
$\dot{v}$	$cm^{-1}\ d$	0.036	20	0.019	20	0.092	20	-	Energy Conductance
κ	-	0.871	-	0.990	-	0.98	-	-	Fraction of Energy Allocated to Soma
$[E_G]$	$J\ cm^{-3}$	5227	-	5077	-	5222	-	-	Volume-specific Cost of Structure
$[\dot{p}_M]$	$J\ cm^{-3}\ d^{-1}$	251.2	20	54.67	20	87.21	20	-	Volume-specific Somatic Maintenance Rate
E_H^b	J	0.108	-	0.0001	-	0.064	-	-	Birth Threshold
E_H^j	J	27.1	-	0.674	-	0.063	-	-	Metamorphosis Threshold
E_H^p	J	8132	-	244	-	544.6	-	-	Puberty Threshold
Ww_i	g	45.45	-	48.47	-	46.68	-	1	Ultimate Wet Weight
L_∞	cm	2.92	-	3.51	-	3.05	-	1	Ultimate Structural Length
δ_M	-	0.207	-	0.166	-	0.159	-	-	Shape Coefficient

*Value taken from *E. encrasicolus* entry

The Arrhenius temperature was estimated to be 6071 K, which indicates *E. japonicus* are less thermally sensitive than *E. encrasicolus* and *E. anchoita*. The fraction of energy allocated to the soma, κ = 0.871, is a typical value for ray-finned fish and less unusual than the values published for the other anchovies (Kooijman *et al.* 2014). The difference in κ explains the difference in the estimated maturity thresholds between *E. japonicus* and the other anchovies. The specific somatic maintenance rate $[\dot{p}_M]$ is much higher than most fishes, but high values of $[\dot{p}_M]$ have been reported for other small pelagic planktivores for which levels of data completeness are similarly high (Kooijman *et al.* 2014). The von Bertalanffy

growth rate $\dot{r}_B$, the growth rate experienced after metabolic acceleration, is also comparatively high (0.009 scaled length per day; see Kooijman 2010 for an explanation of scaled parameters) compared to the other anchovies (0.002 for *E. encrasicolus* and 0.0009 for *E. anchoita*), which can be expected given the high $[\dot{p}_M]$.

Table 4. Comparison of DEB model predictions with observed zero-variate data for female *E. japonicus* at 20°C. All lengths are standard length (SL)

Data	Observation	Prediction	Source
Age at Mouth Opening	3.3 d	3.99 d	Fukuhara (1983)
Age at Metamorphosis	29 d	29.92 d	Takahashi & Watanabe (2004a)
Age at Sexual Maturity	96 d	91.98 d	Yoneda *et al.* (2015)
SL at Mouth-opening	0.335 cm	0.373 cm	Fukuhara (1983)
SL at Metamorphosis	2.64 cm	2.29 cm	Yasue *et al.* (2016)
SL at Sexual Maturity	5.0 – 8.53 cm	8.10 cm	Yoneda *et al.* (2015), Funamoto *et al.* (2004)
Ultimate SL	15.22 cm	14.12 cm	Jung *et al.* (2008)
Ultimate Wet Weight	45 g	45.45	Fadeev (2005)

Comparisons between zero-variate observed data and DEB model predictions can be seen in Table 4. Figures 2 – 7 compare univariate data to predictions made by the DEB model. The DEB model reproduces the age of metamorphosis and sexual maturity, as well as the standard length at mouth opening and sexual maturity quite well. While the estimated standard length at metamorphosis was quite similar to observations by Yasue *et al.* (2016), the underestimation of larval growth seen in figures 3 and 4 suggests that acceleration during the larval stage is not correctly implemented, and this length at metamorphosis value may not be typical for *E. japonicus* in other conditions.

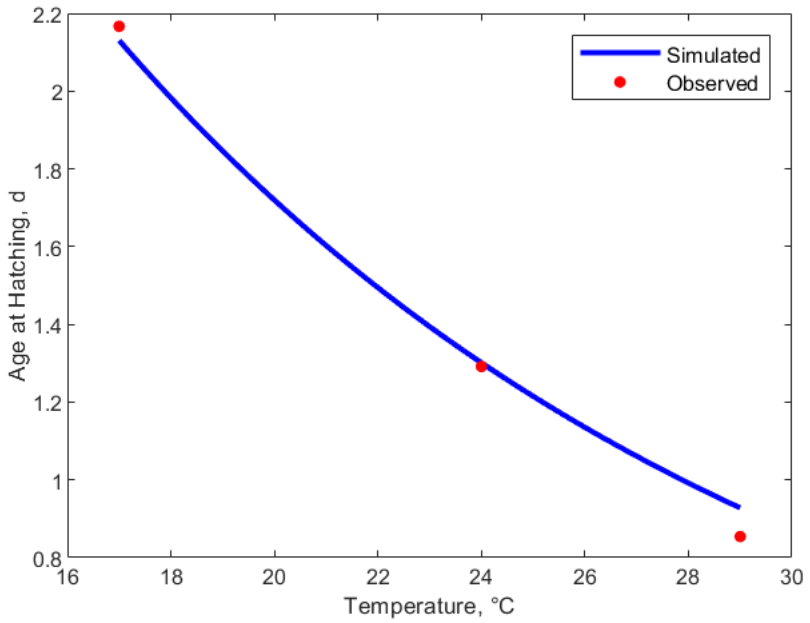

Figure 2. DEB model simulation and observed data for age at hatching (d) of *E. japonicus* eggs at various temperatures (°C) in laboratory conditions (Fukuhara 1983).

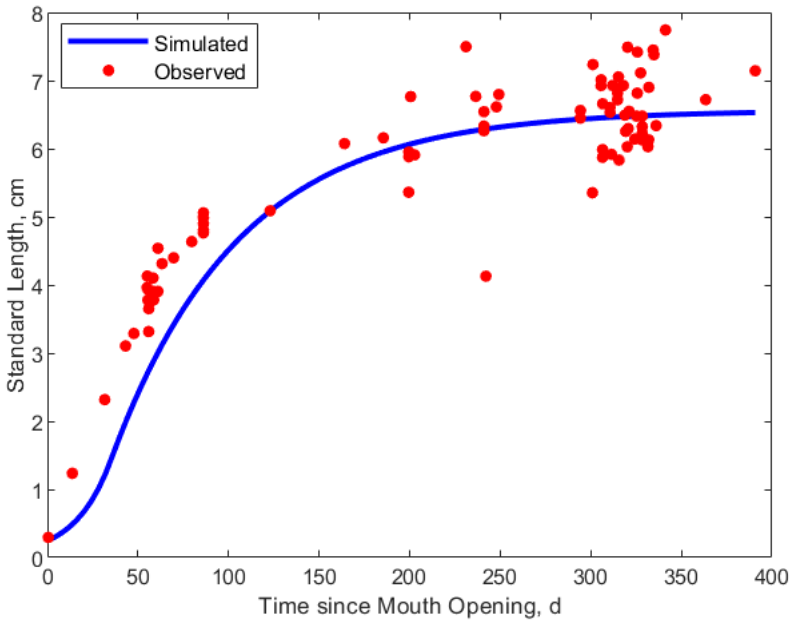

Figure 3. DEB model simulation and observed data for standard length vs. time since mouth opening for anchovy reared in laboratory conditions (Fukuhara and Takao 1988). Thermal conditions during the experiment are described as 'ambient'. The model assumes constant temperature of 22°C. Food density is described as 20 rotifers / mL for days 1-10 and 10 rotifers / mL thereafter. The model assumes food density equivalent to a scaled functional response $f = 0.48$

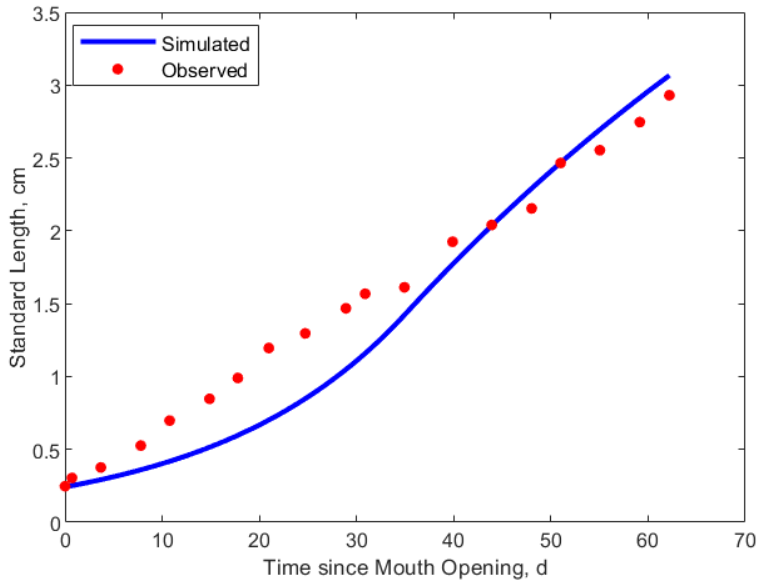

Figure 4. DEB model simulation and observed data for standard length vs. time since mouth opening for anchovy reared in laboratory conditions (Fukuhara 1983). Thermal conditions during the experiment are described as 'ambient'. The model assumes constant temperature of 22°C. Food density is described as 20 rotifers / mL for days 1-10 and 10 rotifers / mL thereafter. The model assumes food density equivalent to a scaled functional response $f = 0.48$.

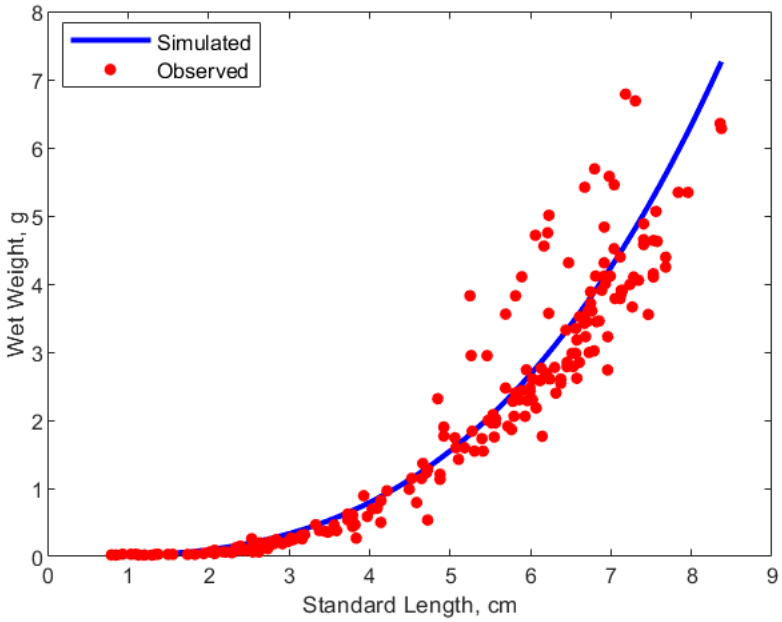

Figure 5. DEB model simulation and observed data for standard length vs. wet weight for anchovy reared in laboratory conditions (Fukuhara and Takao 1988). Food density is described as 20 rotifers / mL for days 1-10 and 10 rotifers / mL thereafter. The model assumes food density equivalent to a scaled functional response $f = 0.48$.

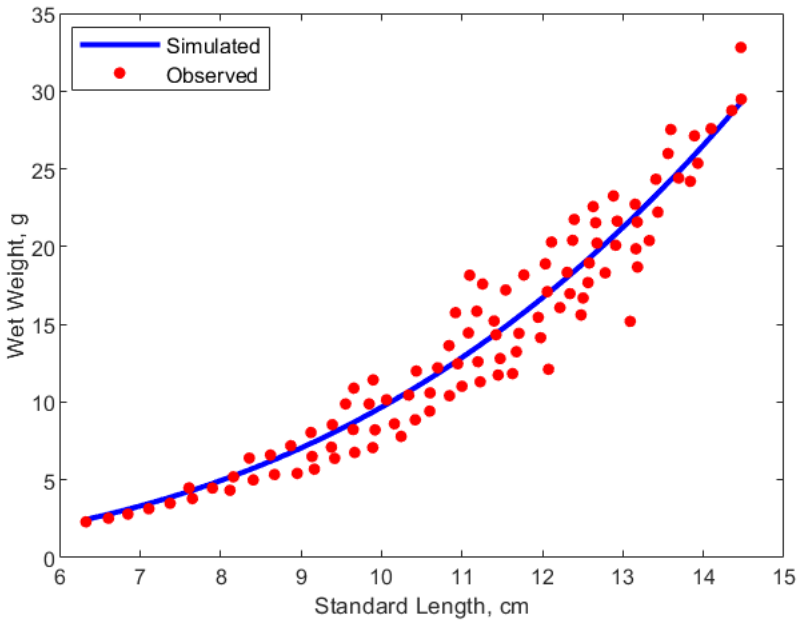

Figure 6. DEB model simulation and observed data for standard length vs. wet weight for anchovy sampled from Wakasa Bay in summer (Funamoto *et al.* 2004). Adult food availability was described as 'low'. The model assumes food density equivalent to a scaled functional response $f = 0.11$.

Table 4 shows the prediction for ultimate wet weight (45.45 g) is similar to the heaviest weight observed (Fadeev 2005), but the prediction for ultimate standard length is clearly underestimated, given anchovies of longer length have been observed even amongst the data used in this study (figure 6). Figure 2 suggests the relationship between hatching time and temperature is being approximated well, as are the growth dynamics of the embryo. With the exception of the under-estimated larval growth, growth as a function of length is predicted satisfactorily (figures 3 & 4) and weight as a function of length (figures 5 & 6) is predicted well, although the food levels assumed by the model in figure 6 are notably low. Figure 7 shows that the reproductive rate as a function of both food and temperature is approximated well, although the reproductive rate at high food levels is overestimated.

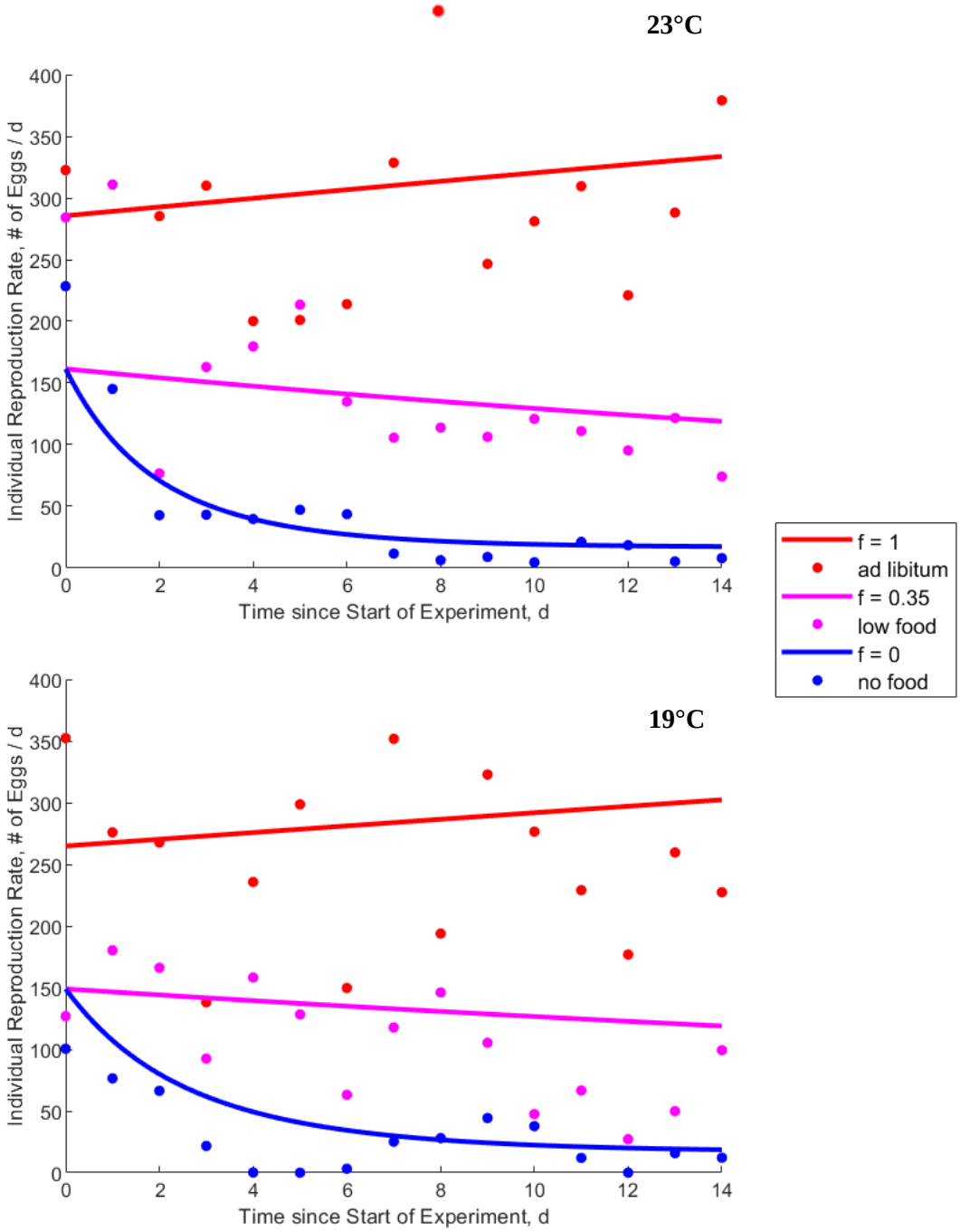

Figure 7. DEB model simulation (solid line) and observed data (points) for the mean number of eggs laid per day by female anchovy at 23°C (top panel) and 19°C (bottom panel) at varying food levels (Yoneda *et al.* 2014). Food treatment described as 'ad libitum' (5% body weight per day, red line), 'low' (1.75% body weight per day, pink line) and 'no food' (blue line). All individuals were fed ad libitum before the onset of the experiment. Average length of individuals at start of experiment = 9 cm SL. The model assumes food density equivalent to a scaled functional response of $f = 1$ (ad libitum), $f = 0.35$ (low food), $f = 0$ (no food). The mean number of eggs laid per individual for day 8 of the 23°C experiment, ad libitum cohort was 523.

3.2 Results of DEB-IBM Model Validation

The DEB-IBM, using DEB parameter values described in the previous section, reproduced patterns of larval growth for *E. japonicus* for spring, summer and winter seasons (Takasuka *et al.* 2017; figures 9 – 11), but not autumn (figure 8).

Larval and early juvenile growth for autumn 2003 was underestimated by the DEB-IBM from day 17 – 50 (figure 8), suggesting real anchovies underwent metabolic acceleration around 20 days before the simulation. For the summer of 2004, observed anchovies appear to undergo metabolic acceleration a few days later than the simulation's prediction (figure 10).

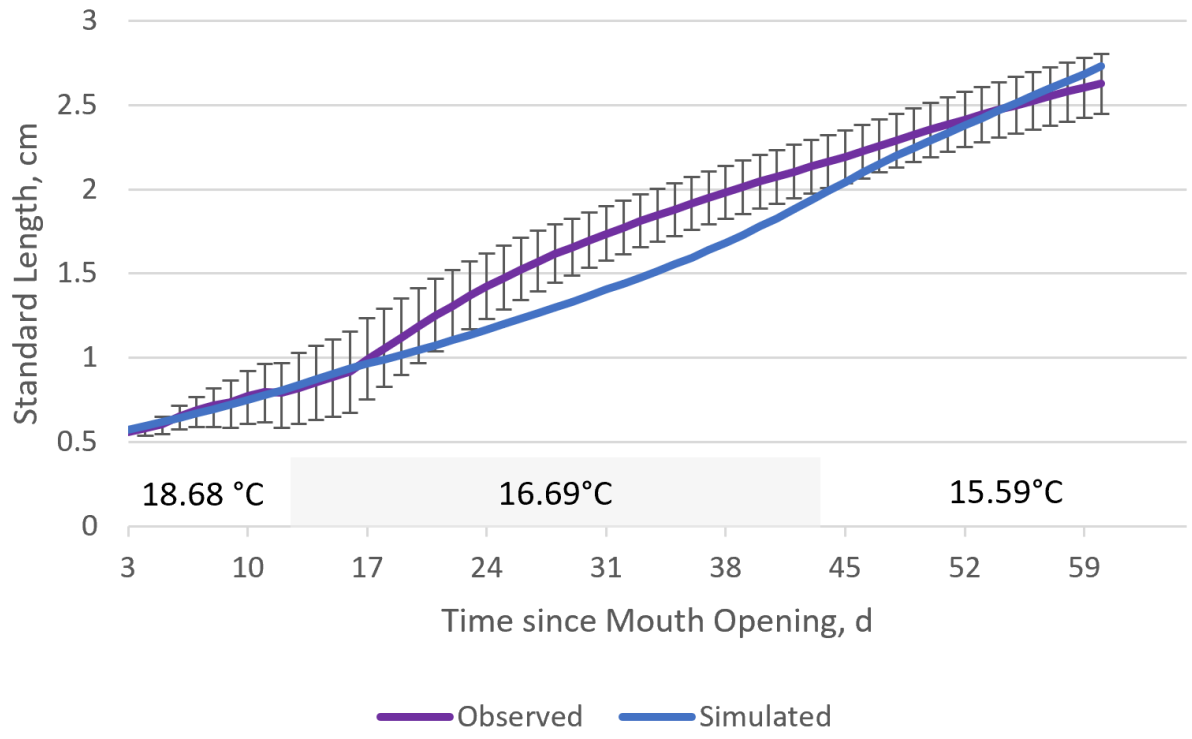

Figure 8. DEB model simulation and observed data for standard length vs. time since mouth opening for anchovy in Sagami Bay, October 19th – December 15th 2003 (Takasuka *et al.* 2017). Error bars represent 95% confidence intervals. The temperature experienced by the anchovies is unknown. Feeding conditions were reported to be 'relatively high'. The DEB-IBM uses historical monthly average sea surface temperatures for Sagami Bay as environmental forcing (temperatures used by the model are as indicated) and assumes ad libitum feeding conditions ($f = 1$).

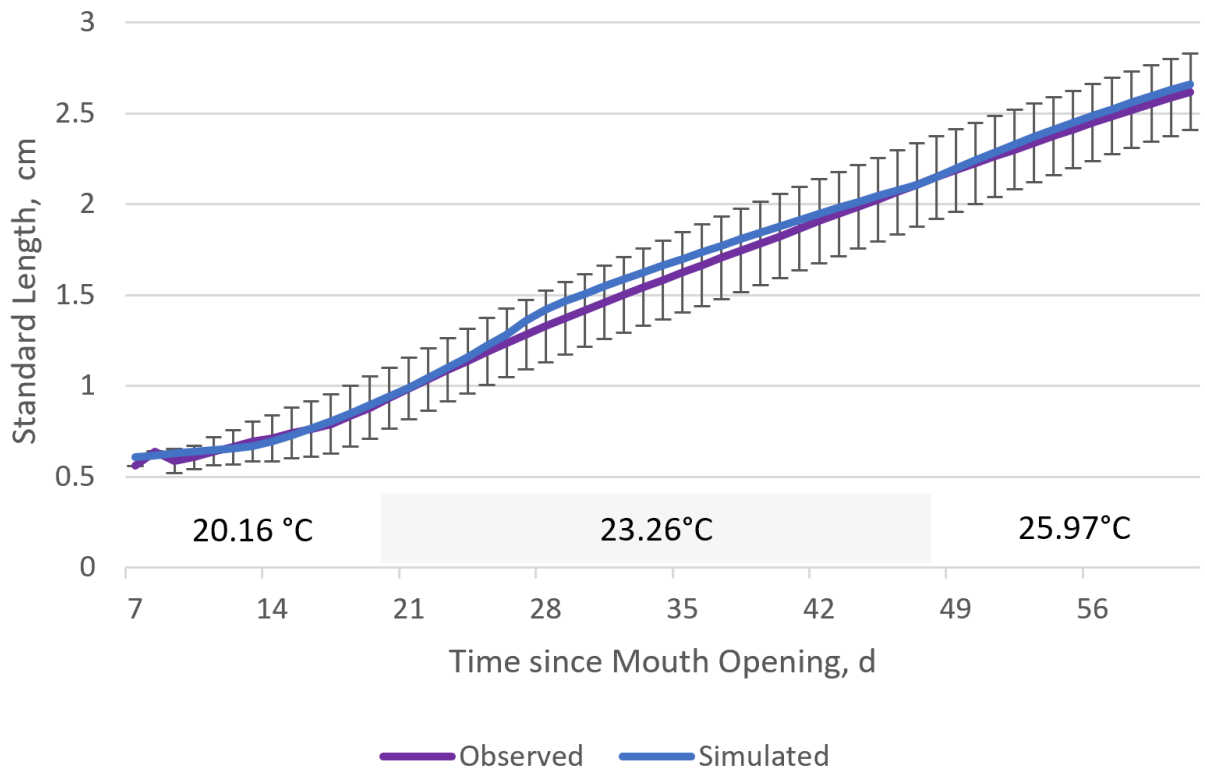

Figure 9. DEB model simulation and observed data for standard length vs. time since mouth opening for anchovy in Sagami Bay, March 13th – May 6th 2004 (Takasuka *et al.* 2017). Error bars represent 95% confidence intervals. The temperature experienced by the anchovies is unknown. Feeding conditions were reported to be 'relatively high'. The DEB-IBM uses historical monthly average sea surface temperatures for Sagami Bay as environmental forcing (temperatures used by the model are as indicated) and assumes ad libitum feeding conditions (f = 1).

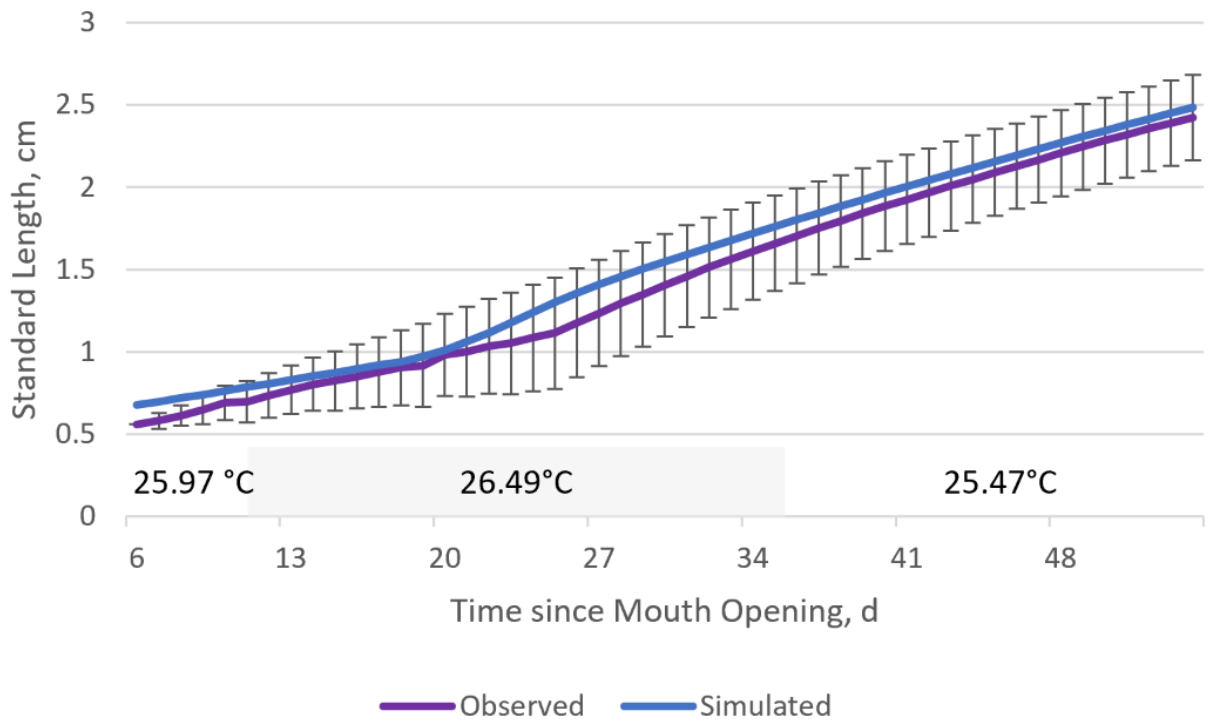

Figure 10. DEB model simulation and observed data for standard length vs. time since mouth opening for anchovy in Sagami Bay, May 27th – July 15th 2004 (Takasuka *et al.* 2017). Error bars represent 95% confidence intervals. The temperature experienced by the anchovies is unknown. Feeding conditions were reported to be 'relatively high'. The DEB-IBM uses historical monthly average sea surface temperatures for Sagami Bay as environmental forcing (temperatures used by the model are as indicated) and assumes ad libitum feeding conditions ($f = 1$).

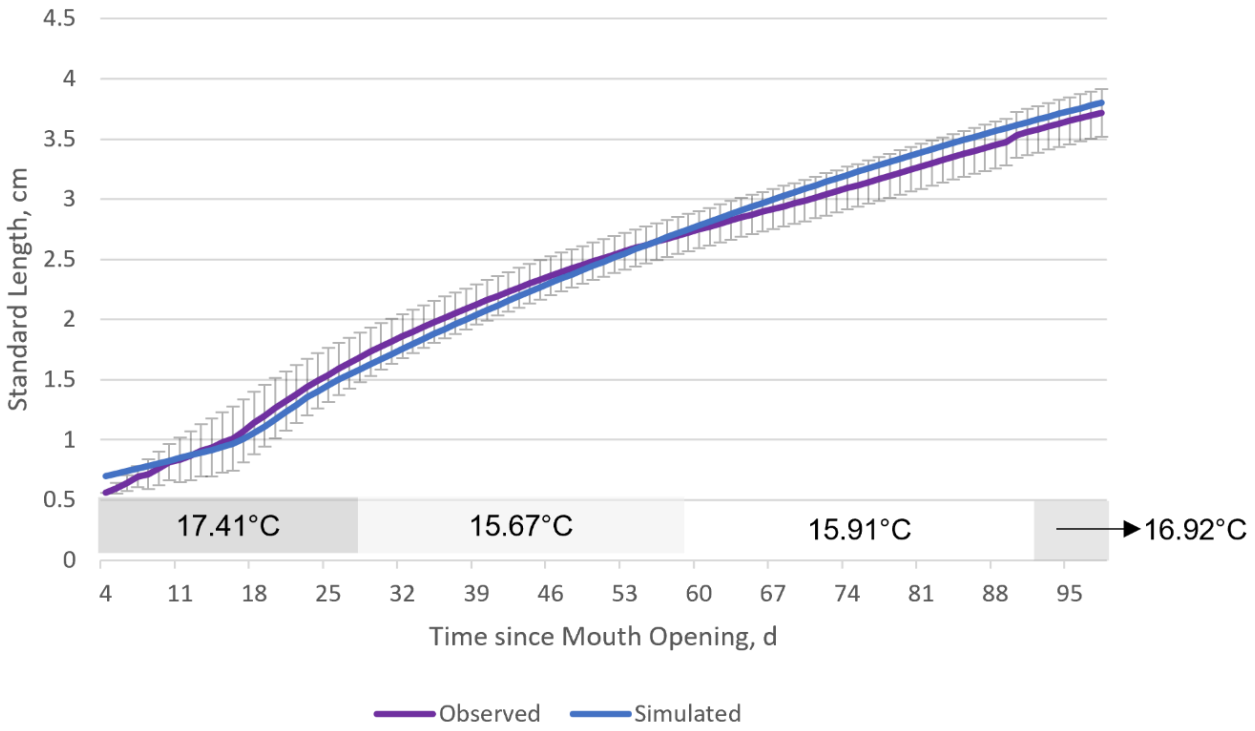

Figure 11. DEB model simulation and observed data for standard length vs. time since mouth opening for anchovy in Sagami Bay, November 13th – February 14th 2005 (Takasuka *et al.* 2017). Error bars represent 95% confidence intervals. The temperature experienced by the anchovies is unknown. Feeding conditions were reported to be 'relatively high'. The DEB-IBM uses historical monthly average sea surface temperatures for Sagami Bay as environmental forcing (temperatures used by the model are as indicated) and assumes ad libitum feeding conditions ($f = 1$).

3.3 Results of DEB-IBM Simulations until 2100

Average monthly potential sea temperature data from 2015 to 2100 were predicted and the average across depths and geographical range of *E. japonicus* was taken (figure 12). An increase of roughly 1.5°C in total mean temperature is expected for the entire range. The sea surface temperature around Japan is thought to have increased by 1.11°C in the past 100 years (Yatsu 2019).

Initial predictions of stock size by the DEB-IBM, based on estimates of eggs laid and egg mortality rates, underpredicted the initial size of the Tsushima Warm Current stock (figure 13), which is thought to be greater than 90,000 tonnes (Tsuya 2019). The DEB-IBM failed to capture stock size dynamics (figure 13). In all simulations the stock size crashed after initial exponential increases.

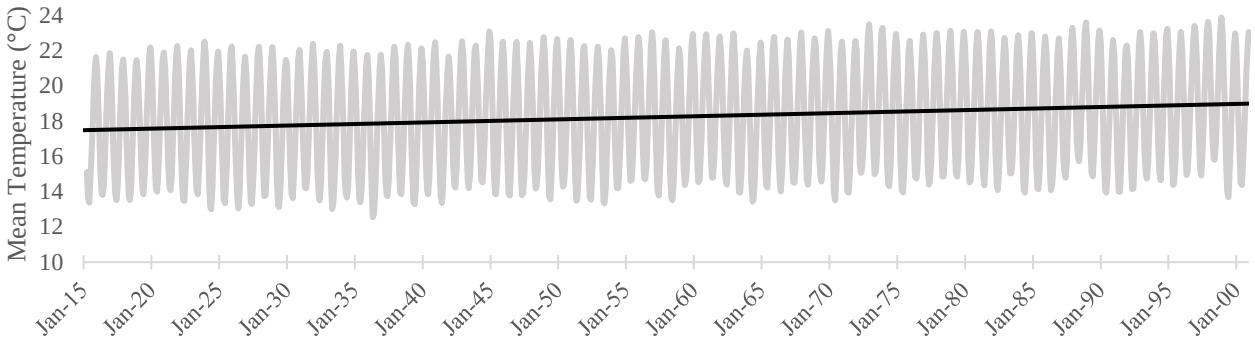

Figure 12. Predicted change in monthly mean potential sea temperature from January 2015 to December 2100, averaged across the geographical range of *E. japonicus* (113°E - 140°E, 21.25°N - 48°N) and depths of 5, 25, 55 and 105 metres. Predicted temperatures were obtained from the World Climate Research Program's Coupled Model Intercomparison Project 6: FIO-ESM-2-0 ssp245 experiment.

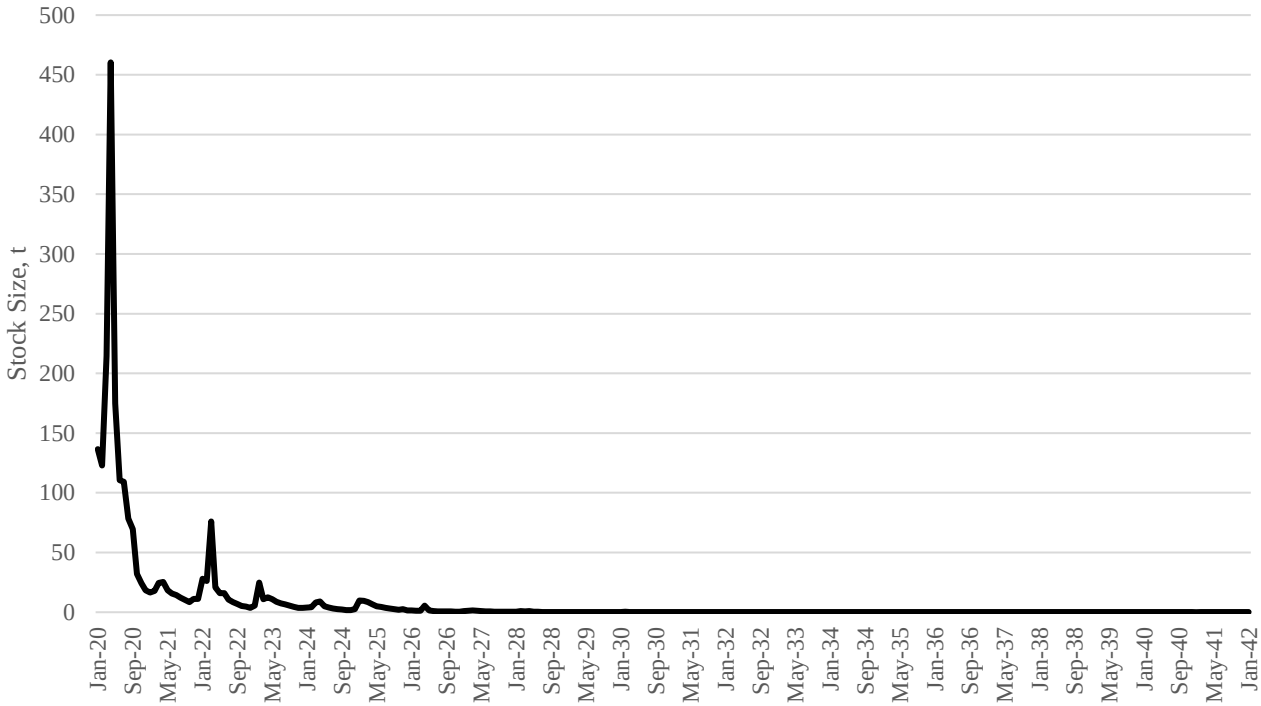

Figure 13. Typical simulation of the Tsushima Warm Current stock by the DEB-IBM, initialised using estimates of egg abundance and mortality. Initial population booms are followed by a crash. The DEB-IBM assumes ad libitum food conditions and temperatures corresponding to figure 13.

The mean length of mature anchovies (~11.5 cm SL) did not change significantly between 2015 and 2100, while the mean structural length at metamorphosis and sexual maturity increased slightly over time (figure 14). The age at completion of metamorphosis and sexual maturity, however, saw relatively strong decreases over time (figure 15).

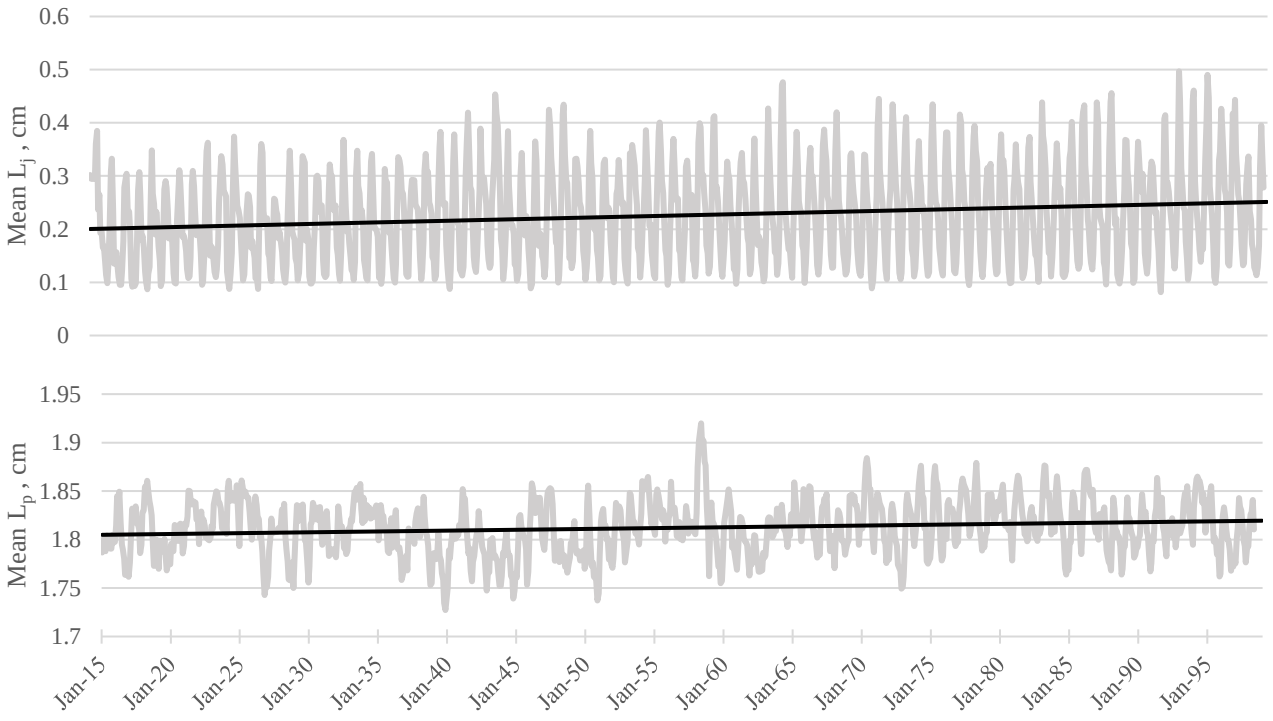

Figure 14. Predicted change in mean structural length at metamorphosis (L_j; top panel) and mean structural length at sexual maturity (L_p; bottom panel) from January 2015 to December 2100. The DEB-IBM assumes ad libitum food conditions and temperatures corresponding to figure 13.

Simulated adults produced an average of 11 batches per year, which is much lower than observations of 36 batches per year reported by Jung *et al.* (2008). The relative batch fecundity was within the observed range (figure 18) and did not change from with mean temperature over time (figure 16). Spawning frequency was observed to increase over time with mean temperature, but the values were much lower than values observed in the literature (figure 19).

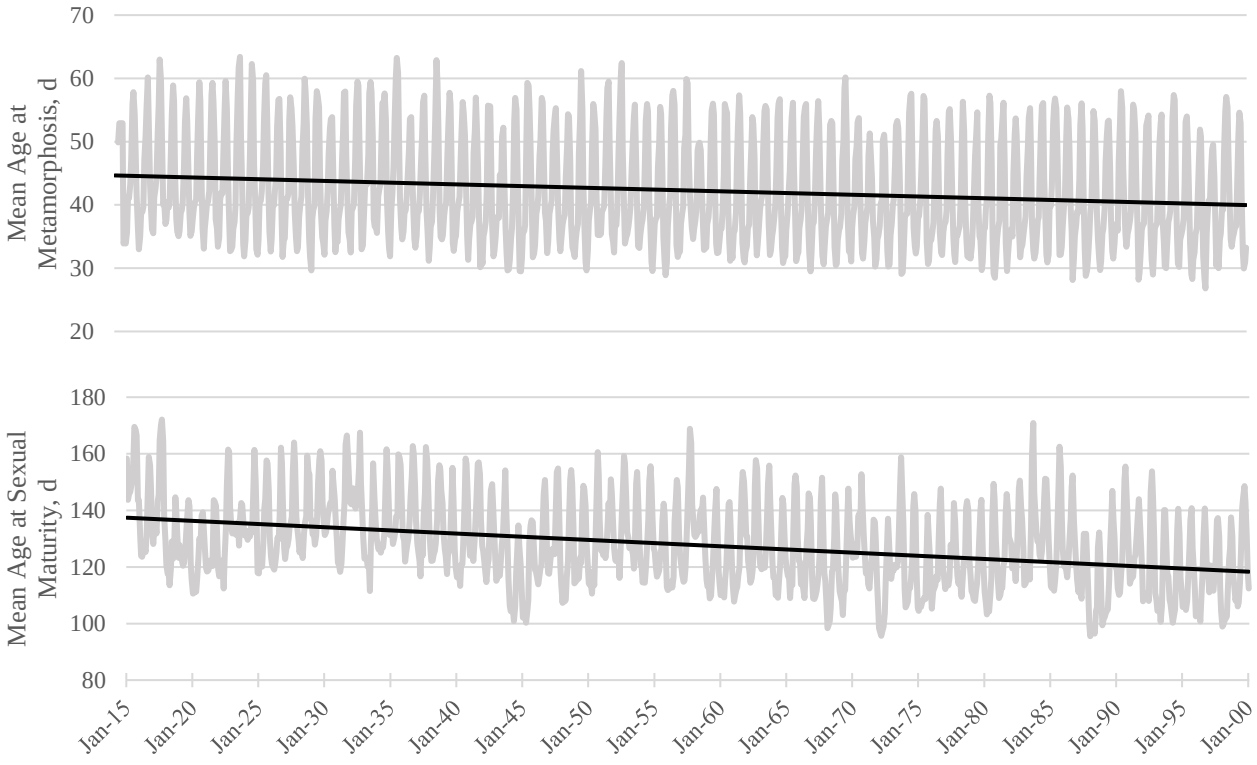

Figure 15. Predicted change in mean age at completion of metamorphosis and mean age at sexual maturation from January 2015 to January 2100. The DEB-IBM assumes ad libitum food conditions and temperatures corresponding to figure 13.

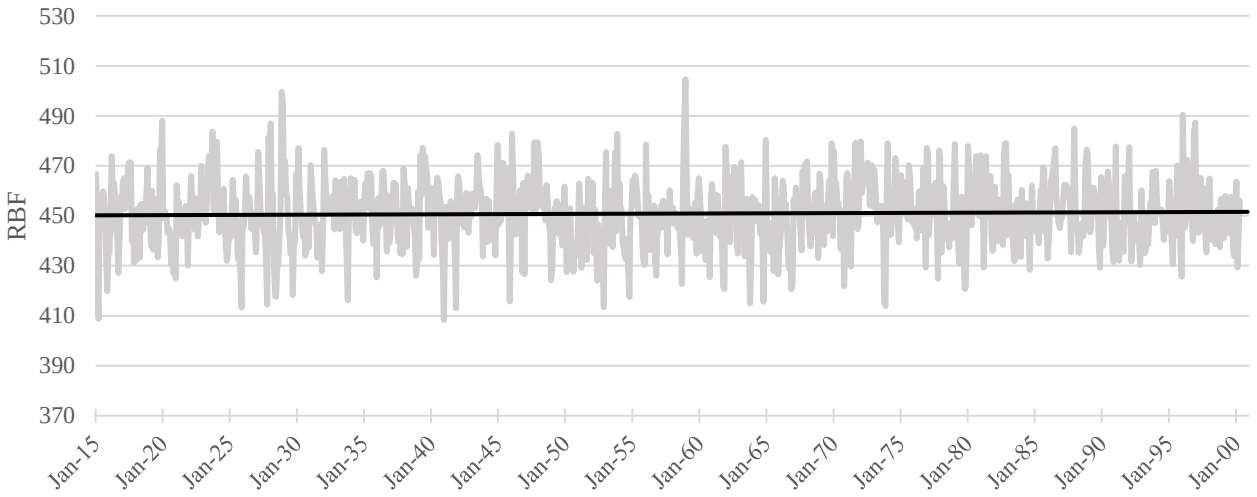

Figure 16. Predicted change in mean relative batch fecundity (RBF; mean number of eggs per gram of somatic body weight) from January 2015 to January 2100. The DEB-IBM assumes ad libitum food conditions and temperatures corresponding to figure 13.

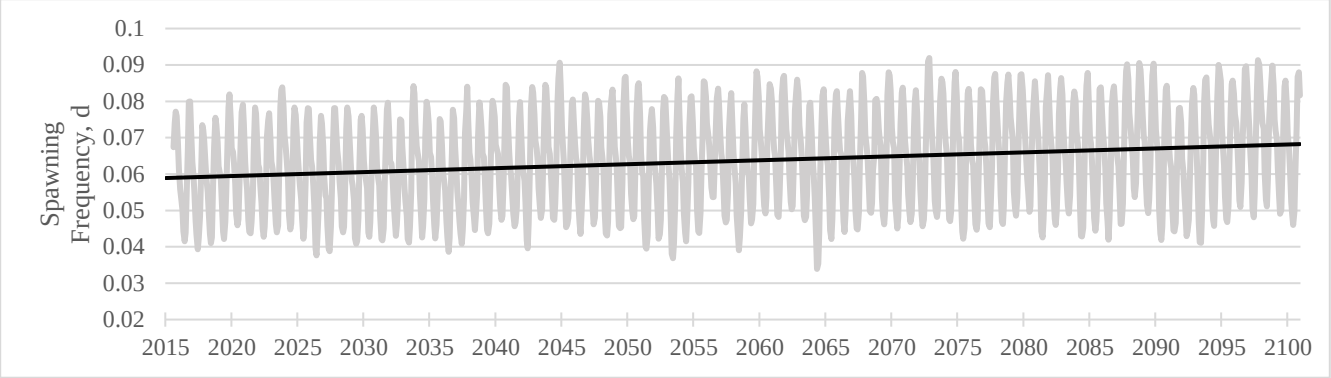

Figure 17. Predicted change in spawning frequency (spawning events per female per day) from January 2015 to January 2100. The DEB-IBM assumes ad libitum food conditions and temperatures corresponding to figure 13.

4 Discussion

4.1 DEB Parameter Values For *E. japonicus*

As shown in table 3, the DEB parameters for *E. japonicus* were estimated and from these predictions of various metabolic processes were calculated. *E. japonicus* was shown to differ from the European *E. encrasicolus* and South American *E. anchoita* in several ways. The lower value of the Arrhenius temperature T_A, which quantifies thermal sensitivity, is not surprising given the broad optimal thermal range (15.6°C – 27.8°C; Takasuka *et al.* 2007) and geographical range (from Russian to southern Chinese waters; Whitehead *et al.* 1988) of *E. japonicus*.

In the suborder Clupeoidei, which includes the genus *Engraulis*, length at sexual maturity L_p tends to increase proportionally with ultimate length L_∞ (Kooijman 2010). The parameter values of *E. japonicus* do not follow this trend: L_∞ for *E. japonicus* is smaller than the other two Engraulids despite having a greater L_p. The smaller prediction for ultimate length is due to *E. japonicus*' exceptionally high somatic maintenance rate compared to the other Engraulids.

4.1.1 Extraordinarily High Somatic Maintenance Rate: Evidence of "Waste-to-Hurry"?

The high value for the volume-specific somatic maintenance rate, $[\dot{p}_M] = 251.2$ $J \cdot cm^{-3}$ structural body mass per day, is unusual but not without precedent: for the similarly-sized and well-documented zebrafish *Danio rerio* $[\dot{p}_M] = 500$ (Augustine *et al.* 2011). Even more comprehensively documented and studied is the water flea *Daphnia magna*, for which $[\dot{p}_M] > 1000$; it is unlikely cellular turnover and physical activity alone can explain such high rates of energy expenditure to the soma (Kooijman 2013). One possible explanation is the "waste-to-hurry" hypothesis, which posits some species respond quickly at the population level to local and brief periods of favourable conditions by keeping their life cycle short (Kooijman 2013). While it is intuitive to think that to reproduce quickly, one should eat quickly and thereby mature quickly, doing so also increases somatic growth. A larger body size necessitates greater amounts of food for survival and further lengthens the life cycle. This can be avoided if an abundance of energy is 'wasted' on somatic maintenance, which consequently reduces energy available for growth. As the "κ rule" of DEB theory dictates (Kooijman 2010), a fixed portion of energy is invested to somatic processes and is distinct from energy allocated to maturation and reproduction. As a result, a high $[\dot{p}_M]$ leads to small-bodied species capable of reaching sexual maturity relatively quickly. Such speedy life cycles could favour timely population responses to temporally favourable conditions.

Indeed, food availability for *E. japonicus* is highly variable for all life stages, as are the physical conditions it experiences across regions, seasons and years (Lindsay *et al.* 1998). The waste-to-hurry hypothesis also offers an explanation for why *E. japonicus* matures relatively quickly compared to *E. encrasicolus*, despite *E. encrasicolus* presumably having greater selective pressure for fast maturation due to the harsh northern winter conditions and accompanying high mortality experienced by its young (REF). It should be noted, however, that the data used to estimate the age of sexual maturity were obtained from a rearing experiment with ad libitum food conditions and a temperature of 20°C (Yoneda *et al.* 2015), and therefore may not well represent the age of sexual maturity experienced in the wild.

4.1.2 Inaccurate Prediction of Growth in the Early Stages

For the most part, the estimated DEB parameters approximate observations of *E. japonicus* well, including embryo dynamics and quantification of temperature (figure 2), the weight-length relationship (figures 5 & 6) and reproduction rate as a function of food and temperature (figure 7).

Growth rate during the larval stage and early juvenile stage was underestimated, specifically between SL of 0.5 – 4.5 cm (age 5 – 100 days; figure 3) and 0.5 – 2 cm (age 5 – 35 days; figure 4). There are two possible, interrelated reasons for this period of growth underestimation: an inaccurate estimate of the length at metamorphosis, or the failure to implement a shape coefficient specific to the larval stage.

The length at metamorphosis L_j is an important parameter because it determines to what extent metabolic acceleration occurs. The acceleration factor, which is multiplied by the assimilation rate and energy conductance to allow exponential growth during the larval stage, is equal to $\mathcal{M}(L) = \frac{L}{L_b}$ until reaching its maximum $s_{\mathcal{M}} = \frac{L_j}{L_b}$. Thus, a greater L_j will lead to a greater disparity between metabolic
rates post-metamorphosis and pre-metamorphosis, as well as a steeper growth curve during the larval stage.

The observed length at completion of metamorphosis used to predict L_j in this study, 2.64 cm SL (Yasue *et al.* 2016) is smaller than reported elsewhere (e.g. 3.7 cm; Takahashi & Watanabe 2004a), although the length at certain life stages is highly variable in *E. japonicus* (Funamoto *et al.* 2004, Yoneda *et al.* 2015). It is also possible that metamorphosis *sensu* DEB theory, which simply marks the end of metabolic acceleration, is not analogous to metamorphosis often reported in the literature, usually defined by the completion of guanine deposition on the peritoneal surface (Takahashi & Watanabe 2004a, Yasue *et al.* 2016). If metamorphosis, and therefore L_j, were instead defined as the point at which exponential growth becomes von Bertalanffy growth, itself a highly variable metric but observed to occur around 55 days (Takahashi & Watanabe 2004a, 2004b), then simulated growth during early stages may better replicate the steep growth curves observed in figure 3.

The underestimation of larval growth rates seen in figure 4, and to a lesser degree the initial portion of the curve in figure 3, can be explained by the lack of a shape coefficient specific to the larval stage. The shape coefficient δ_M converts structural length to physical (i.e. measurable) length, e.g. standard length. The DEB model assumed *E. japonicus* to be isomorphs, organisms who do not change shape and have a constant δ_M throughout ontogeny, with a $\delta_M = 0.207$. Given the poor estimation of larval growth, *E. japonicus* may actually be 'V1 morphs', species who change shape throughout ontogeny and whose physical length during the larval stage is defined with a dynamic shape coefficient: $\delta_M = \delta_{Mb} * w_b + \delta_{Mj} + w_j$, where δ_{Mb} and δ_{Mj} are the shape coefficients at birth and metamorphosis, $w_b = \frac{L_{j-L}}{L_j - L_b}$ and $w_j = 1 - w_b$. While *E. japonicus* do not outwardly show signs of shape change (Fukuhara 1983), it is possible allometric-like growth of non-visible components of structure, such as the digestive organs, could justify the inclusion of a V1-morphic shape correction.

Indeed, the inclusion of a shape coefficient that follows V1-morphy in the DEB-IBM better approximates growth, discussed in the following section.

4.2 DEB-IBM Model Validation

Larval growth rate is an important metric to predict accurately because it is a predictor of survival rate (Takahashi & Watanabe 2004b, Takasuka *et al.* 2003). Presumably, faster growth allows larvae to escape the intense predation pressure experienced at small sizes more quickly (Takahashi & Watanabe 2002). Knowing recruitment rates can elucidate reasons for stock size fluctuations, which is valuable knowledge for the sustainable harvest of fishery resources and understanding how stock dynamics will be affected by climate change (Fréon *et al.* 2006).

Using the newly-estimated DEB parameter values and including V1-morphic shape correction to account for changes in shape during larval growth, the DEB-IBM successfully recreated patterns of growth in *E. japonicus* from Sagami Bay across seasons (figures 9 – 11). Larval growth rates were within the range of values reported elsewhere, 0.03 – 0.07 cm per day (Yasue & Takasuka 2009, Takahashi & Watanabe 2004b).

It was found that the structural length upon completion of metamorphosis, L_j, was specific to each season's cohort: a constant L_j led to simulations that failed to reproduce observed growth. Body length is more closely linked to the timing of metamorphosis than age, and reliance of the DEB-IBM on cohort-specific L_j values suggests that the timing and duration of metamorphosis varies across seasons and cohorts, in line with previous observations (Takahashi & Watanabe 2004a).

4.2.1 Temperature and Growth

Although dynamic environmental forcing was limited to broad spatial and temporal averages of sea temperature, the DEB-IBM satisfactorily predicted larval growth. This suggests temperature is the primary environmental predictor of *E. japonicus* larval growth rates, corroborating previous findings (Takasuka & Aoki 2002, Takasuka & Aoki 2006, Yasue & Takasuka 2009). The effect of temperature on larval and juvenile growth of *E. japonicus* is complex and not yet definitively understood. While growth is generally positively correlated temperature, other environmental factors can limit growth even when temperature conditions are favourable (Takahashi & Watanabe 2005). Indeed, it is possible that thermal conditions deemed ideal in physiological studies may in reality indirectly affect food or other environmental conditions in the wild in a way that is unfavourable for larval growth. This may explain the dome-shaped relationship between growth and temperature previously reported (Takasuka *et al.* 2007, Hwang *et al.* 2006). However, recent evidence suggests the negative effect of warm temperatures on larval growth rates are only observed in specific locations during the summer (Yu *et al.* 2020, Xing *et al.* 2021). This may be related to the effects of temperature on food availability.

4.2.2 Food Availability and Growth

While the effect of food density on larval growth rates has been non-significant in some instances (Takasuka & Aoki 2006, Yasue & Takasuka 2009), other studies have suggested that food density can be a limiting factor for growth of *E. japonicus* larvae when food conditions are not optimal (Takahashi & Watanabe 2005, Takasuka & Aoki 2006, Zenitani *et al.* 2009). The results of the DEB-IBM seem to support this: the overestimation of larval growth seen in the summertime simulation (figure 10) is negated when the food density is lowered from $f = 1$ (i.e. maximum food availability) to $f = 0.85$ (85% maximum). The period for which lower food availability predicts growth better corresponds to a particularly warm period (figure 17), which corroborates the conjecture that food availability can become limited in summers of high sea temperature (Yamamoto *et al.* 2018). High summer temperatures could limit food availability through biotic or abiotic means: nutrient transport systems in *E. japonicus* summer grounds can be inhibited through stratification, and important local prey species have difficulty surviving at temperatures approaching 27°C (Xing *et al.* 2021).

The DEB-IBM's close fit with observations from Sagami Bay suggest food availability for larvae there is close to ad libitum for the seasons assessed. However, food availability is suspected to be more limited, and therefore play a more significant role in larval and juvenile growth rates, in the Pacific offshore (Takahashi & Watanabe 2005) and East China Sea (Takasuka & Aoki 2006). It is therefore possible that the DEB-IBM would overpredict anchovy growth and recruitment success for offshore waters without explicit incorporation dynamic food levels as environmental forcing input.

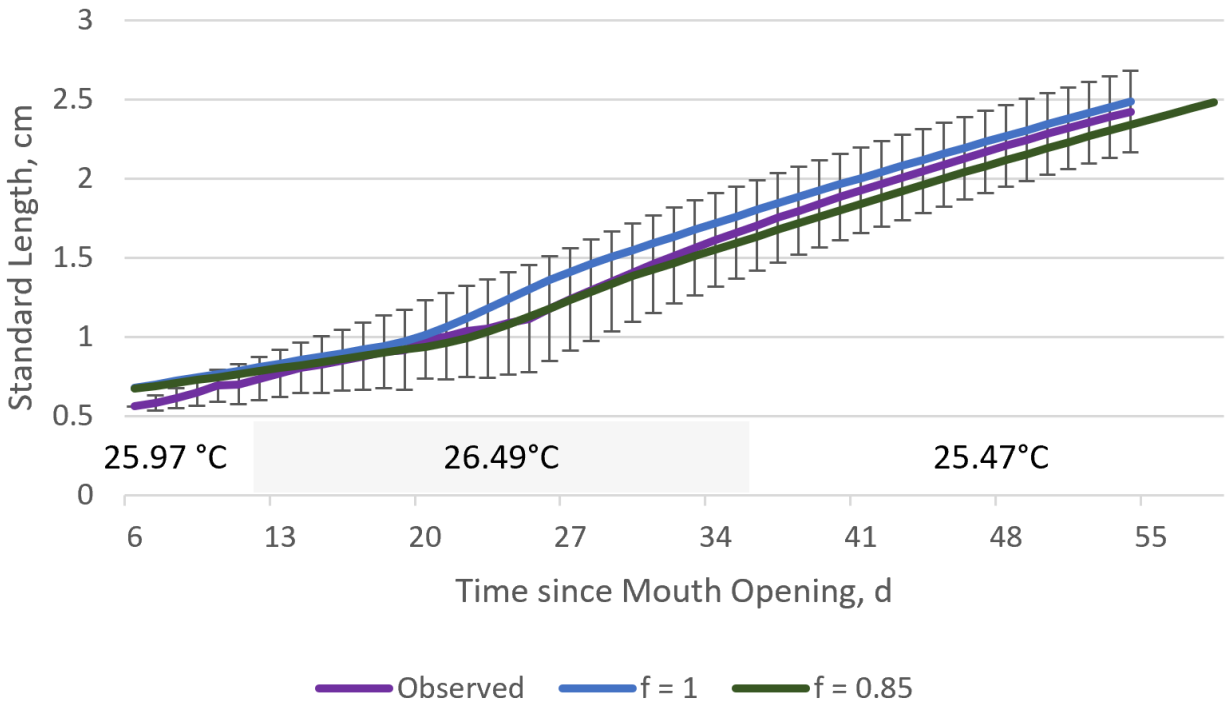

Figure 18. DEB model simulations assuming ad libitum feeding conditions and 85% ad libitum feeding conditions, compared to observed data for standard length vs. time since mouth opening for anchovy in Sagami Bay, May 27th – July 15th 2004 (Takasuka *et al.* 2017). Error bars represent 95% confidence intervals. The temperature experienced by the anchovies is unknown. Feeding conditions were reported to be 'relatively high'. The DEB-IBM uses historical monthly

average sea surface temperatures for Sagami Bay as environmental forcing (temperatures used by the model are as indicated.

4.3 DEB-IBM Simulations until 2100

4.3.1 Patterns in Growth and Length

The mean length of mature anchovies was not affected by the long-term increase in mean sea temperature from 2015 – 2100. Feeding conditions affect ultimate length while temperature does not (Kooijman 2010). As individuals approach their ultimate length and growth becomes minimal, the effects of temperature on observed length-at-age also become minimal.

The length at metamorphosis and length at sexual maturity are primarily functions of growth rate, which is temperature-dependent (figure 15). The simulations here follow observations in the literature that high temperatures cause metamorphosis and sexual maturation to occur at smaller sizes (Yoneda *et al.* 2015). Differences in thermal regimes may explain wide variation in reported standard length at sexual maturity between locations: 6 cm in Sagami Bay (Funamoto 2001), 7.38 cm in Osaka Bay and 8.53 cm in Wakasa Bay (Funamoto *et al.* 2004) and 5.0 cm (26.8°C) and 6.6 cm (20.8°C) in ad libitum laboratory conditions (Yoneda *et al.* 2015). Smaller size at sexual maturity would allow anchovy to reproduce in a shorter timeframe and may be an advantageous adaption to increasingly variable environmental conditions. However, associated increases in egg mortality would likely ultimately reduce recruitment rates (Wan and Bian 2012).

4.3.2 Stock Dynamics

The stock of *E. japonicus* has decreased across all regions of the Northwest Pacific in recent years (Yatsu *et al.* 2019). However, the DEB-IBM's results failed to capture trends in stock size that reflect reality. This is likely due to the limitations of the DEB-IBM's population size, which was capped at 100 SIs due to limitations of computational power. This limits the variability present in the population and makes it more susceptible to synchronisation and crashes, which is what can be observed in figure 13. Running the model without a population cap and with realistic food conditions would be more likely to elucidate mechanisms that determine observed patterns in *E. japonicus* stock size.

4.3.3 Trends in Fecundity and Spawning

E. japonicus is a prolific spawner with a highly variable spawning season: just 2 months in subarctic waters to year-round in some Japanese coastal areas (Suhara *et al.* 2004). The spawning season is most often recorded as spring to autumn (Hayashi 1966, Tsuruta & Hirose 1989). The minimum temperature required for spawning seems to be 15°C, but spawning may not occur at warmer temperatures if food is insufficient (Funamoto *et al.* 2004). Long spawning seasons are hypothesised to maximise the chance of encountering favourable conditions for offspring. This trait compliments the

observation of a high somatic maintenance rate for *E. japonicus*; both describe a life history selected to adapt quickly to variable environments.

The RBF of *E. japonicus* varies greatly across seasons, years, regions and study methodologies, indicating reproductive ecology adapts to local conditions. Several mechanisms have been proposed for such variation and are likely not mutually exclusive. The results of the DEB-IBM show no long-term correlation between temperature and RBF (figure 16), which supports previous laboratory findings for laboratory-reared anchovy fed ad libitum, where no relationship was found between RBF and temperature (Yoneda *et al.* 2014).

The variation in reported values of RBF (figure 18) are likely due differences across locations and seasons in intertwined contributing factors such as food availability, temperature and spawning season length. For instance, the high RBF reported for subarctic regions by Suhara *et al.* (2013) could be intuitively explained by the food-rich waters coupled with a short spawning season. Takasuka *et al.* (2005) reported RBF to decrease with temperature, quickly for inshore anchovies and more gradually in offshore waters. When food conditions are less than optimal in cooler waters, it is possible anchovies allocate the same proportion of energy into fewer, larger eggs to increase the chance of survival (Yoneda *et al.* 2014). Indeed, smaller egg sizes are associated with increased mortality (Wan & Bian 2012), and egg size is negatively correlated with temperature (Imai & Tanaka 1997, Wan & Bian 2012). However, a positive correlation between RBF and temperature has also been reported (Imai & Tanaka 1997). In conditions of low food availability associated with warmer temperatures, anchovies seem to control RBF by reducing egg size and energy content (Tsuruta 1992). Such a strategy could be advantageous in conditions of low food availability, as numerous energy-poor eggs would likely face greater chance of survival than fewer energy-rich eggs. Increasing fecundity in *E. japonicus* stocks (Imai & Tanaka 1997, Zeng *et al.* 2005) coupled with evidence of decreasing mean length and age (Li *et al.* 2006) are thought to be driving factors of increased egg mortality and subsequent reductions to recruitment over the past half century (Wan and Bian 2012). Given the DEB-IBM predicts a continuation of these trends, it is possible recruitment of anchovy will continue to decline over the next century.

The total fecundity, in this study represented by the number of batches produced per year, was grossly underestimated. It is possible that the reproduction data used to estimate the DEB parameters (see figure 7) are not representative of *E. japonicus* populations in the wild, possibly due to the stress of rearing experiments, misconceptions of which food conditions constitute ad libitum feeding for *E. japonicus*, or other aspects of experimental setup. More data on fecundity at known food conditions would improve the accuracy of the DEB parameters in this regard.

The spawning frequencies predicted by the DEB-IBM are within ranges observed within the literature (figure 19). Spawning frequency is highest in summer and lowest in winter, in line with evidence that egg development is faster at higher temperatures (Yoneda *et al.* 2015). The temperature-dependence of spawning frequency may differ between onshore and offshore groups: inshore groups share a spawning frequency with offshore groups at temperatures 5°C warmer (Takasuka *et al.* 2005), again suggesting a high degree of local adaptation in *E. japonicus*.

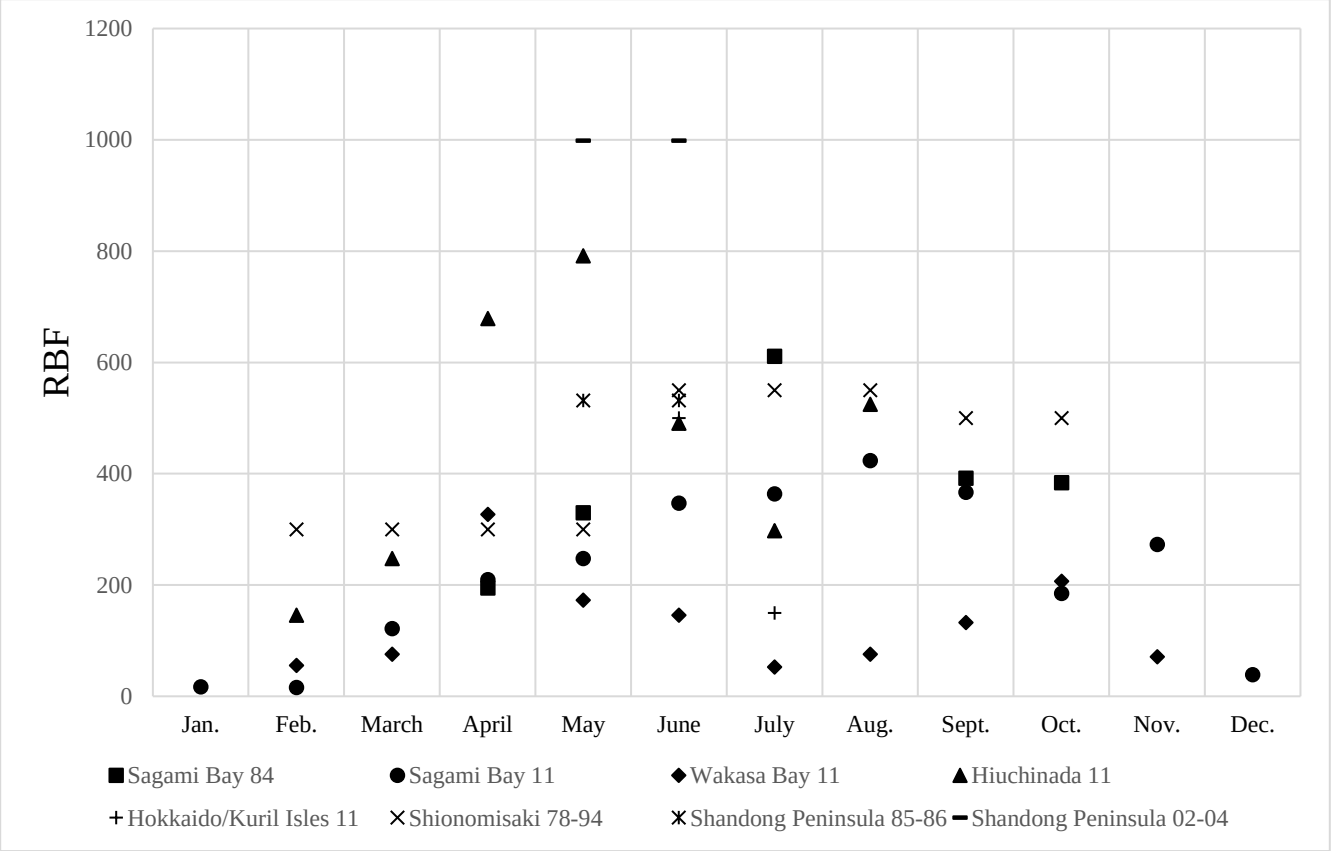

Figure 19. Variation in relative batch fecundity (RBF; # of eggs per spawning event per gram of total body weight) for *E. japonicus* across seasons and regions in the Northwest Pacific. The values from Feb. – May, June – August and Sept. – Oct. for Shionomisaki are mean values from 1978 – 1994. The values from May – June for Shandong Peninsula are mean values from 1985 – 1986 and 2002 – 2004. Sources: Sagami Bay 84 (Tsuruta 1992); Sagami Bay 11, Wakasa Bay, Hiuchinada, Hokkaido/Kuril Isles (Suhara *et al.* 2014); Shionomisaki (Okada & Wada 1992); Shandong Peninsula (Zeng *et al.* 2005).

Food availability is positively correlated with spawning frequency (Tsuruta 1992, Yoneda *et al.* 2015). It is likely some of the variation seen in figure 19 is due to food availability's co-dependency with seasonal temperatures.

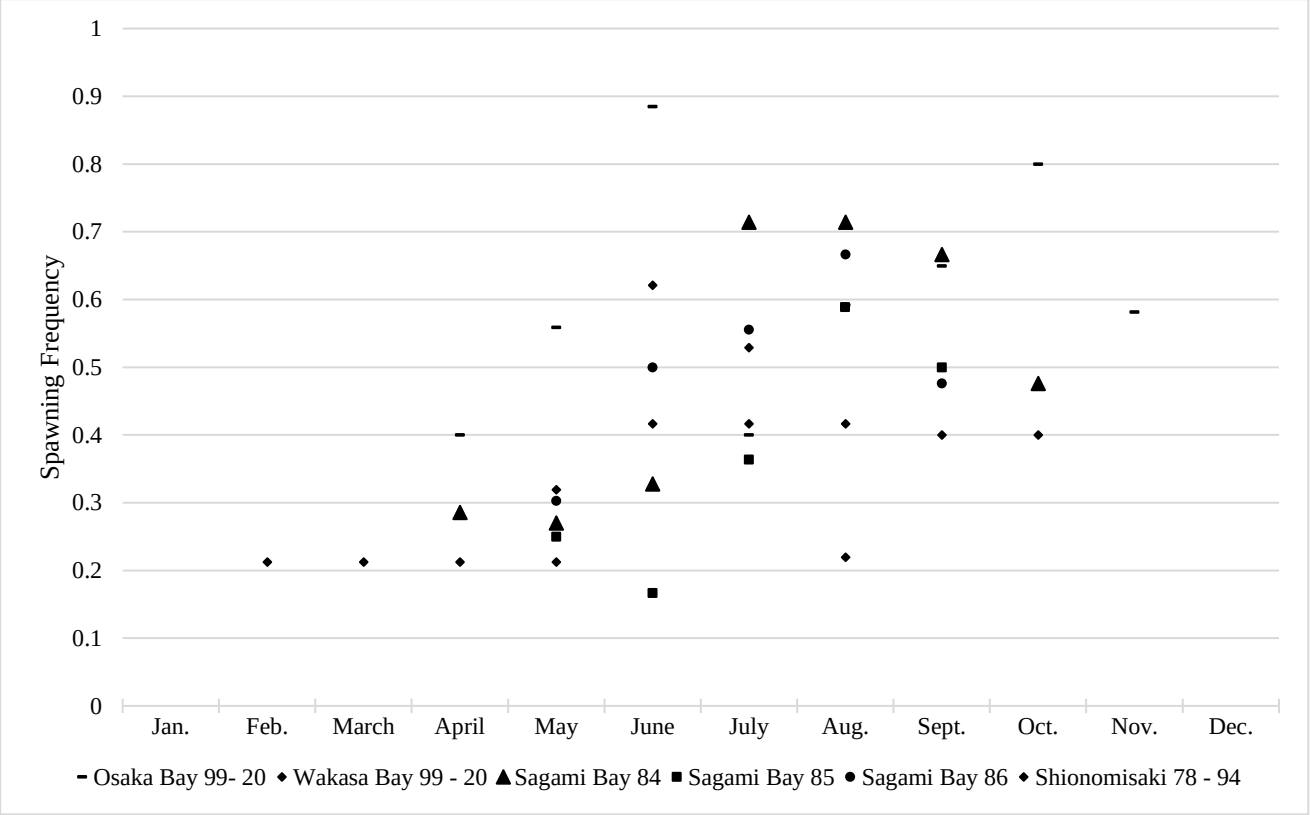

Figure 20. Variation in spawning frequency (# of spawning events per day during spawning season) for *E. japonicus* across seasons and regions in the Northwest Pacific. The values from Feb. – May, June – August and Sept. – Oct. for Shionomisaki are mean values from 1978 – 1994. Sources: Osaka Bay, Wakasa Bay (Funamoto *et al.* 2004); Sagami Bay (Tsuruta 1992); Shionomisaki (Okada & Wada 1992).

4.4 Limitations of this Study

The DEB-IBM was limited in several ways. First, monthly mean temperature, averaged across the entire Northwest Pacific and across depths up to 105 metres, is a poor indicator of the actual temperatures experienced by anchovy on a daily basis. The DEB-IBM built in this study is a tool for predicting possible long-term physiological shifts resulting from changes in mean environmental conditions. There is growing consensus in the literature, however, that mean conditions are less biologically relevant than extreme conditions or the variability of such conditions (Morash *et al.* 2018, Denny 2017). A future study at a finer temporal and spatial scale, with thermal variability encountered by anchovy day-to-day implemented, would be an ideal next step. Although computationally demanding and data intensive, such an endeavour would produce results of greater ecological meaning.

Food is a key determinant in body size, reproductive output and many other important life history attributes. The assumption made by the DEB-IBM, that food conditions are optimal, does not represent conditions experienced in the wild. Obtaining future forecasts of phytoplankton abundance, and using such data to quantitatively predict zooplankton abundance, could be a good first step towards integrating dynamic food levels as environmental forcing input to improve the accuracy and realism of forecasts.

Lastly, the data used to parameterise the DEB model could be further expanded upon. In particular, more reproductive data and growth data during the larval stage, at specified food and temperature levels, would allow a more confident estimation of annual fecundity and the length at metamorphosis *sensu* DEB, which would improve predictions of larval growth and eliminate the need to fix L_j for each cohort. More data at known food levels and temperature could also be used to better estimate the shape coefficient, further enabling accuracy of larval growth and length.

5 Conclusion

An array of data from the literature was used to estimate the DEB parameters for *Engraulis japonicus.* The values of the DEB parameters suggest *E. japonicus* is highly adaptive, can tolerate a wide range of temperatures and allocates a relatively high amount of energy to reproduction. The results of parameterisation suggest a high volume-specific somatic maintenance rate $[\dot{p}_M]$, which may indicate an inefficient metabolism that selects for quicker population responses to environmental fluctuations through the mechanism of reduced body size.

The DEB-IBM was able to replicate the dynamics of larval growth but only if the value of the length at metamorphosis was manually fit to each curve. This suggests that the duration of metabolic acceleration, i.e. the period of exponential growth, depends on the unique conditions experienced by each cohort of larvae. More data on larval growth at known food and temperature conditions would allow a more accurate estimate of the length at metamorphosis and would improve predictions of larval growth across seasons and locations.

DEB-IBM simulations run until the year 2100 under a scenario of moderate climate change indicate several changes to *E. japonicus* life history. While the length at sexual maturity and metamorphosis is not expected to change, the age at which these events occur is expected to decrease, suggesting a trend towards faster development and a shorter lifecycle. This is supported by the prediction of increased spawning frequency. While the ultimate size of anchovy is not expected to increase due to ocean warming, growth and size could be hindered by food shortages related to high summer temperatures, as the literature and results of this study suggest. Relative batch fecundity is not expected to change, although eggs are likely to become smaller and less energy dense, resulting in increased egg mortality rates.

Literature Cited

Augustine, S., Gagnaire, B., Floriani, M., Adam-Guillermin, C., & Kooijman, S. A. L. M. (2011). Developmental energetics of zebrafish, Danio rerio. *Comparative Biochemistry and Physiology - A Molecular and Integrative Physiology*, *159*(3), 275–283. https://doi.org/10.1016/j.cbpa.2011.03.016

Bao, Y., Song, Z., & Qiao, F. (2020). FIO-ESM Version 2.0: Model Description and Evaluation. *Journal of Geophysical Research: Oceans*, *125*(6), 1–21. https://doi.org/10.1029/2019JC016036

Brander, K. (2015). Improving the Reliability of Fishery Predictions Under Climate Change. In *Current Climate Change Reports* (Vol. 1, Issue 1, pp. 40–48). Springer. https://doi.org/10.1007/s40641-015-0005-7

Bueno-Pardo, J., Petitgas, P., Kay, S., & Huret, M. (2020). Integration of bioenergetics in an individual-based model to hindcast anchovy dynamics in the Bay of Biscay. *ICES Journal of Marine Science*, *77*(2), 655–667. https://doi.org/10.1093/icesjms/fsz239

Chavez, F. P., Ryan, J., Lluch-Cota, S. E., & Ñiquen, C. M. (2003). Climate: From anchovies to sardines and back: Multidecadal change in the Pacific Ocean. *Science*, *299*(5604), 217–221. https://doi.org/10.1126/science.1075880

Cheung, W. W. L., Lam, V. W. Y., Sarmiento, J. L., Kearney, K., Watson, R., & Pauly, D. (2009). Projecting global marine biodiversity impacts under climate change scenarios. *Fish and Fisheries*, *10*(3), 235–251. https://doi.org/10.1111/j.1467-2979.2008.00315.x

Cury, P., Bakun, A., Crawford, R. J. M., Jarre, A., Quiñones, R. A., Shannon, L. J., & Verheye, H. M. (2000). Small pelagics in upwelling systems: Patterns of interaction and structural changes in "wasp-waist" ecosystems. *ICES Journal of Marine Science*, *57*(3), 603–618. https://doi.org/10.1006/jmsc.2000.0712

Denny, M. (2017). The fallacy of the average: On the ubiquity, utility and continuing novelty of Jensen's inequality. In *Journal of Experimental Biology* (Vol. 220, Issue 2, pp. 139–146). Company of Biologists Ltd. https://doi.org/10.1242/jeb.140368

Enders, E. C., & Boisclair, D. (2016). Effects of environmental fluctuations on fish metabolism: Atlantic salmon Salmo salar as a case study. *Journal of Fish Biology*, *88*(1), 344–358. https://doi.org/10.1111/jfb.12786

Fukuhara, O. (1983). Development and growth of laboratory reared Engraulis japonica (Houttuyn) larvae. *Journal of Fish Biology*, *23*(6), 641–652. https://doi.org/10.1111/j.1095-8649.1983.tb02943.x

Funamoto, T., Aoki, I., & Wada, Y. (2004). Reproductive characteristics of Japanese anchovy, Engraulis japonicus, in two bays of Japan. *Fisheries Research*, *70*(1), 71–81. https://doi.org/10.1016/j.fishres.2004.06.017

Grimm, V., Berger, U., Deangelis, D. L., Polhill, J. G., Giske, J., & Railsback, S. F. (2010). The ODD protocol: A review and first update. *Ecological Modelling*, *221*, 2760–2768. https://doi.org/10.1016/j.ecolmodel.2010.08.019

Hayasi, S. (1961). A note on the biology and fishery of the japanese anchovy. *CalCOFI, XI*, 44–57.

Hwang, S. D., Song, M. H., Lee, T. W., McFarlane, G. A., & King, J. R. (2006). Growth of larval Pacific anchovy Engraulis japonicus in the Yellow Sea as indicated by otolith microstructure analysis. *Journal of Fish Biology*, *69*(6), 1756–1769. https://doi.org/10.1111/j.1095-8649.2006.01244.x

Imai, C., & Tanaka, S. (1997). Effect of Sea Water Temperature on Variability of Batch Fecundity in Japanese Anchovy from Coastal Waters around Miura Peninsula, Central Japan. *Fisheries Science*, *63*(4), 489–495. https://doi.org/10.2331/fishsci.63.489

Jung, S., Hwang, S. Do, & Kim, J. (2008). Fecundity and growth-dependent mortality of Pacific anchovy (Engraulis japonicus) in Korean coastal waters. *Fisheries Research*, *93*(1–2), 39–46. https://doi.org/10.1016/j.fishres.2008.02.004

Jusup, M., Sousa, T., Domingos, T., Labinac, V., Marn, N., Wang, Z., & Klanjšček, T. (2017). Physics of metabolic organization. *Physics of Life Reviews*, *20*, 1–39. https://doi.org/10.1016/j.plrev.2016.09.001

Kim, J., & Lo, N. C. H. (2001). Temporal variation of seasonality of egg production and the spawning biomass of Pacific anchovy, Engraulis japonicus, in the southern waters of Korea in 1983-1994. *Fisheries Oceanography*, *10*(3), 297–310. https://doi.org/10.1046/j.1365-2419.2001.00175.x

Kooijman, S. A. L. M., Hoeven, N. Van Der, & Werf, D. C. Van Der. (1989). Population Consequences of a Physiological Model for Individuals. *Functional Ecology*, *3*(3), 325. https://doi.org/10.2307/2389373

Kooijman, S. A. L. M. (2013). Waste to hurry: Dynamic energy budgets explain the need of wasting to fully exploit blooming resources. *Oikos*, *122*(3), 348–357. https://doi.org/10.1111/j.1600-0706.2012.00098.x

Kooijman, S. A. L. M. (2014). Metabolic acceleration in animal ontogeny: An evolutionary perspective. *Journal of Sea Research*, *94*, 128–137. https://doi.org/10.1016/j.seares.2014.06.005

Kooijman, S. A. L. M. (2009). Dynamic energy budget theory for metabolic organisation, third edition. In *Dynamic Energy Budget Theory for Metabolic Organisation, Third Edition*. https://doi.org/10.1017/CBO9780511805400

Kooijman, S. A. L. M., Pecquerie, L., Augustine, S., & Jusup, M. (2011). Scenarios for acceleration in fish development and the role of metamorphosis. *Journal of Sea Research*, *66*(4), 419–423. https://doi.org/10.1016/j.seares.2011.04.016

Kooijman, S. A. L. M. (2020). The standard dynamic energy budget model has no plausible alternatives. *Ecological Modelling*, *428*(January), 109106. https://doi.org/10.1016/j.ecolmodel.2020.109106

Kooijman, S. A. L. M., & Lika, K. (2014). Comparative energetics of the 5 fish classes on the basis of dynamic energy budgets. *Journal of Sea Research*, *94*, 19–28. https://doi.org/10.1016/j.seares.2014.01.015

Kuwae, M., Yamamoto, M., Sagawa, T., Ikehara, K., Irino, T., Takemura, K., Takeoka, H., & Sugimoto, T. (2017). Multidecadal, centennial, and millennial variability in sardine and anchovy abundances in the western North Pacific and climate–fish linkages during the late Holocene. *Progress in Oceanography*, *159*(August 2016), 86–98. https://doi.org/10.1016/j.pocean.2017.09.011

Lenton, T., Rockström, J., Gaffney, O., Rahmstorf, S., Richardson, K., Steffen, W., & Shellnhuber, H. J. (2019). Climate tipping points - too risky to bet against. *Nature*, *575*(7784), 592–595. https://doi.org/10.1038/d41586-019-03595-0

Lika, K., Kearney, M. R., Freitas, V., van der Veer, H. W., van der Meer, J., Wijsman, J. W. M., Pecquerie, L., & Kooijman, S. A. L. M. (2011). The "covariation method" for estimating the parameters of the standard Dynamic Energy Budget model I: Philosophy and approach. *Journal of Sea Research*, *66*(4), 270–277. https://doi.org/10.1016/j.seares.2011.07.010

Lindsay, D. J., Minagawa, M., Mitani, I., & Kawaguchi, K. (1998). Trophic Shift in the Japanese Anchovy Engraulis japonicus in its Early Life History Stages as Detected by Stable Isotope Ratios in Sagami Bay, Central Japan. *Fisheries Science*, *64*(3), 403–410. https://doi.org/10.2331/fishsci.64.403

Liu, S., Liu, Y., Alabia, I. D., Tian, Y., Ye, Z., Yu, H., Li, J., & Cheng, J. (2020). Impact of Climate Change on Wintering Ground of Japanese Anchovy (Engraulis japonicus) Using Marine Geospatial Statistics. *Frontiers in Marine Science*, *7*(July), 1–15. https://doi.org/10.3389/fmars.2020.00604

Marques, G. M., Augustine, S., Lika, K., Pecquerie, L., Domingos, T., & Kooijman, S. A. L. M. (2018). The AmP project: Comparing species on the basis of dynamic energy budget parameters. *PLOS Computational Biology*, *14*(5), e1006100. https://doi.org/10.1371/journal.pcbi.1006100

Marques, G. M., Lika, K., Augustine, S., Pecquerie, L., & Kooijman, S. A. L. M. (2019). Fitting multiple models to multiple data sets. *Journal of Sea Research*, *143*(June 2018), 48–56. https://doi.org/10.1016/j.seares.2018.07.004

Martin, B. T., Zimmer, E. I., Grimm, V., & Jager, T. (2012). Dynamic Energy Budget theory meets individual-based modelling: A generic and accessible implementation. *Methods in Ecology and Evolution*, *3*(2), 445–449. https://doi.org/10.1111/j.2041-210X.2011.00168.x

Martin, B., Zimmer, E., Grimm, V., Jager, T., & Year, J. T. (2012). *DEB-IBM: Model Description Dynamic Energy Budget theory meets individual-based modelling: a generic and accessible implementation The rationale of the model and its implementation are explained in: Dynamic Energy Budget theory meets individ-ual-based mode*.

Muhling, B. A., Brodie, S., Smith, J. A., Tommasi, D., Gaitan, C. F., Hazen, E. L., Jacox, M. G., Auth, T. D., & Brodeur, R. D. (2020). Predictability of Species Distributions Deteriorates Under Novel Environmental Conditions in the California Current System. *Frontiers in Marine Science*, *7*(July), 1–22. https://doi.org/10.3389/fmars.2020.00589

Nakayama, S. I., Takasuka, A., Ichinokawa, M., & Okamura, H. (2018). Climate change and interspecific interactions drive species alternations between anchovy and sardine in the western North Pacific: Detection of causality by convergent cross mapping. *Fisheries Oceanography*, *27*(4), 312–322. https://doi.org/10.1111/fog.12254

Naman, S. M., Rosenfeld, J. S., Neuswanger, J. R., Enders, E. C., & Eaton, B. C. (2019). Comparing correlative and bioenergetics-based habitat suitability models for drift-feeding fishes. *Freshwater Biology*, *64*(9), 1613–1626. https://doi.org/10.1111/fwb.13358

Nisbet, R. M., Jusup, M., Klanjscek, T., & Pecquerie, L. (2012). Integrating dynamic energy budget (DEB) theory with traditional bioenergetic models. *Journal of Experimental Biology*, *215*(6), 892–902. https://doi.org/10.1242/jeb.059675

Niu, M., & Wang, J. (2017). Variation in the distribution of wintering anchovy Engraulis japonicus and its relationship with water temperature in the central and southern Yellow Sea. *Chinese Journal of Oceanology and Limnology*, *35*(5), 1134–1143. https://doi.org/10.1007/s00343-017-6134-1

Okada, Y., & Wada, T. (1992). Reproductive relationships of the Pacific Stock of Japanese Anchovy Engraulis japonicus. *Chem. Pharm. Bull.*, *40*(6), 1569–1572.

Pecquerie, L., Petitgas, P., & Kooijman, S. A. L. M. (2009). Modeling fish growth and reproduction in the context of the Dynamic Energy Budget theory to predict environmental impact on anchovy spawning duration. *Journal of Sea Research*, *62*(2–3), 93–105. https://doi.org/10.1016/j.seares.2009.06.002

Raab, K., Llope, M., Nagelkerke, L. A. J., Rijnsdorp, A. D., Teal, L. R., Licandro, P., Ruardij, P., & Dickey-Collas, M. (2013). Influence of temperature and food availability on juvenile European anchovy Engraulis encrasicolus at its northern boundary. *Marine Ecology Progress Series*, *488*, 233–245. https://doi.org/10.3354/meps10408

Robertson, M. P., Peter, C. I., Villet, M. H., & Ripley, B. S. (2003). Comparing models for predicting species' potential distributions: A case study using correlative and mechanistic predictive modelling techniques. *Ecological Modelling*, *164*(2–3), 153–167. https://doi.org/10.1016/S0304-3800(03)00028-0

Rougier, T., Lassalle, G., Drouineau, H., Dumoulin, N., Faure, T., Deffuant, G., Rochard, E., & Lambert, P. (2015). The combined use of correlative and mechanistic species distribution models benefits low conservation status species. *PLoS ONE*, *10*(10), 1–21. https://doi.org/10.1371/journal.pone.0139194

Scheffer, M., Baveco, J. M., DeAngelis, D. L., Rose, K. A., & van Nes, E. H. (1995). Super-individuals a simple solution for modelling large populations on an individual basis. *Ecological Modelling*, *80*(2–3), 161–170. https://doi.org/10.1016/0304-3800(94)00055-M

Sousa, T., Domingos, T., Poggiale, J. C., & Kooijman, S. A. L. M. (2010). Dynamic energy budget theory restores coherence in biology. *Philosophical Transactions of the Royal Society B: Biological Sciences*, *365*(1557), 3413–3428. https://doi.org/10.1098/rstb.2010.0166

Suhara, M., Mori, Y., Mihara, Y., Yamamoto, M., Kawabata, A., Takahashi, M., Katsukawa, Y., Katayama, S., Yamashita, Y., Kawamura, T., & Watanabe, Y. (2013). Comparison of reproductive traits of Japanese anchovy Engraulis japonicus among sea areas around Japan. *Nippon Suisan Gakkaishi (Japanese Edition)*, *79*(5), 813–822. https://doi.org/10.2331/suisan.79.813

Sumaila, U. R., Cheung, W. W. L., Lam, V. W. Y., Pauly, D., & Herrick, S. (2011). Climate change impacts on the biophysics and economics of world fisheries. In *Nature Climate Change* (Vol. 1, Issue 9, pp. 449–456). https://doi.org/10.1038/nclimate1301

Sunday, J. M., Bates, A. E., & Dulvy, N. K. (2012). Thermal tolerance and the global redistribution of animals. *Nature Climate Change*, *2*(9), 686–690. https://doi.org/10.1038/nclimate1539

Takahashi, M., & Watanabe, Y. (2004). Staging larval and early juvenile Japanese anchovy based on the degree of guanine deposition. *Journal of Fish Biology*, *64*(1), 262–267. https://doi.org/10.1111/j.1095-8649.2004.00283.x

Takahashi, M., & Watanabe, Y. (2004). Growth rate-dependent recruitment of Japanese anchovy Engraulis japonicus in the Kuroshio - Oyashio transitional waters. *Marine Ecology Progress Series*, *266*(Pannella 1971), 227–238. https://doi.org/10.3354/meps266227

Takahashi, M., & Watanabe, Y. (2005). Effects of temperature and food availability on growth rate during late larval stage of Japanese anchovy (Engraulis japonicus) in the Kuroshio-Oyashio transition region. *Fisheries Oceanography*, *14*(3), 223–235. https://doi.org/10.1111/j.1365-2419.2005.00334.x

Takasuka, A., & Aoki, I. (2002). Growth rates of larval stage of Japanese anchovy *Engraulis japonicus* and environmental factors in the Kuroshio Extension and Kuroshio-Oyashio transition regions, western North Pacific Ocean. *Fisheries Science*, *68*(sup1), 445–446. https://doi.org/10.2331/fishsci.68.sup1_445

Takasuka, A., & Aoki, I. (2006). Environmental determinants of growth rates for larval Japanese anchovy Engraulis japonicus in different waters. *Fisheries Oceanography*, *15*(2), 139–149. https://doi.org/10.1111/j.1365-2419.2005.00385.x

Takasuka, A., Sakai, A., & Aoki, I. (2017). Dynamics of growth-based survival mechanisms in japanese anchovy (Engraulis japonicus) larvae. *Canadian Journal of Fisheries and Aquatic Sciences*, *74*(6), 812–823. https://doi.org/10.1139/cjfas-2016-0120

Takeshige, A., Miyake, Y., Nakata, H., Kitagawa, T., & Kimura, S. (2015). Simulation of the impact of climate change on the egg and larval transport of Japanese anchovy (Engraulis japonicus) off Kyushu Island, the western coast of Japan. *Fisheries Oceanography*, *24*(5), 445–462. https://doi.org/10.1111/fog.12121

Teal, L. R., Marras, S., Peck, M. A., & Domenici, P. (2018). Physiology-based modelling approaches to characterize fish habitat suitability: Their usefulness and limitations. *Estuarine, Coastal and Shelf Science*, *201*, 56–63. https://doi.org/10.1016/j.ecss.2015.11.014

Tsuruta. (1992). カタクチイワシの成熟・産卵と再生産力の調節に関する研究. 129–168.

Tsuruta, Y. (1991). Reproduction in the Japanese anchovy (Engraulis japonica) as related to Population Fluctuation. *National Research Institute of Fisheries Engineering*, *13*, 129–168.

Urtizberea, A., Fiksen, Folkvord, A., & Irigoien, X. (2008). Modelling growth of larval anchovies including diel feeding patterns, temperature and body size. *Journal of Plankton Research*, *30*(12), 1369–1383. https://doi.org/10.1093/plankt/fbn090

Wan, R., & Bian, X. (2012). Size variability and natural mortality dynamics of anchovy Engraulis japonicus eggs under high fishing pressure. *Marine Ecology Progress Series*, *465*, 243–251. https://doi.org/10.3354/meps09795

Wang, Y., Wei, H., & Kishi, M. J. (2013). Coupling of an individual-based model of anchovy with lower trophic level and hydrodynamic models. *Journal of Ocean University of China*, *12*(1), 45–52. https://doi.org/10.1007/s11802-013-1901-x

Whitehead, P. J. P., Nelson, G. J., & Wongratana, T. (1988). FAO species catalogue. vol 7. clupeoid fishes of the world (Engraulidae). An annotated and ilustrated catalogue of the herrings, sardines, pilchards, sprats, shads anchovies and wolf-herrings. *FAO Fisheries Synopsis*, *7*(2), 305–579.

Xing, Q., Yu, H., Ito, S. ichi, Ma, S., Yu, H., Wang, H., Tian, Y., Sun, P., Liu, Y., Li, J., & Ye, Z. (2021). Using a larval growth index to detect the environment-recruitment relationships and its linkage with basin-scale climate variability: A case study for Japanese anchovy (Engraulis japonicus) in the Yellow Sea. *Ecological Indicators*, *122*, 107301. https://doi.org/10.1016/j.ecolind.2020.107301

Yamamoto, K., Saito, M., & Yamashita, Y. (2018). Relationships between the daily growth rate of Japanese anchovy Engraulis japonicus larvae and environmental factors in Osaka Bay, Seto Inland Sea, Japan. *Fisheries Science*, *84*(2), 373–383. https://doi.org/10.1007/s12562-018-1178-5

Yasue, N., & Takasuka, A. (2009). Seasonal variability in growth of larval Japanese anchovy Engraulis japonicus driven by fluctuations in sea temperature in the Kii Channel, Japan. *Journal of Fish Biology*, *74*(10), 2250–2268. https://doi.org/10.1111/j.1095-8649.2009.02238.x

Yasue, N., Harada, S., & Takasuka, A. (2016). Seasonal variability in the development of Japanese anchovy during the transition from larval to juvenile stages. *Marine Ecology Progress Series*, *562*, 135–146. https://doi.org/10.3354/meps11942

Yatsu, A. (2019). Review of population dynamics and management of small pelagic fishes around the Japanese Archipelago. *Fisheries Science*, *85*(4), 611–639. https://doi.org/10.1007/s12562-019-01305-3

Yoneda, M., Kitano, H., Selvaraj, S., Matsuyama, M., & Shimizu, A. (2013). Dynamics of gonadosomatic index of fish with indeterminate fecundity between subsequent egg batches: Application to Japanese anchovy Engraulis japonicus under captive conditions. *Marine Biology*, *160*(10), 2733–2741. https://doi.org/10.1007/s00227-013-2266-9

Yoneda, M., Kitano, H., Tanaka, H., Kawamura, K., Selvaraj, S., Ohshimo, S., Matsuyama, M., & Shimizu, A. (2014). Temperature- and income resource availability-mediated variation in reproductive investment in a multiple-batch-spawning Japanese anchovy. *Marine Ecology Progress Series*, *516*, 251–262. https://doi.org/10.3354/meps10969

Yoneda, M., Kitano, H., Tanaka, H., Kawamura, K., Selvaraj, S., Ohshimo, S., Matsuyama, M., & Shimizu, A. (2014). Temperature- and income resource availability-mediated variation in reproductive investment in a multiple-batch-spawning Japanese anchovy. *Marine Ecology Progress Series*, *516*(c), 251–262. https://doi.org/10.3354/meps10969

Yoneda, M., Yamamoto, M., Yamada, T., Takahashi, M., & Shima, Y. (2015). Temperature-induced variation in sexual maturation of Japanese anchovy Engraulis japonicus. *Journal of the Marine Biological Association of the United Kingdom*, *95*(6), 1271–1276. https://doi.org/10.1017/S0025315415000405

Yu, H., Yu, H., Ito, S. ichi, Tian, Y., Wang, H., Liu, Y., Xing, Q., Bakun, A., & Kelly, R. M. (2020). Potential environmental drivers of Japanese anchovy (Engraulis japonicus) recruitment in the Yellow Sea. *Journal of Marine Systems*, *212*, 103431. https://doi.org/10.1016/j.jmarsys.2020.103431

Zenitani, H., & Kono, N. (2012). Daily growth rate model of Japanese anchovy larvae Engraulis japonicus in Hiuchi-nada Sea, central Seto Inland Sea. *Fisheries Science*, *78*(5), 1001–1011. https://doi.org/10.1007/s12562-012-0532-2

Zenitani, H., Kono, N., Tsukamoto, Y., & Masuda, R. (2009). Effects of temperature, food availability, and body size on daily growth rate of Japanese anchovy engraulis japonicus larvae in Hiuchi-nada. *Fisheries Science*, *75*(5), 1177–1188. https://doi.org/10.1007/s12562-009-0147-4

Zhao, X., Hamre, J., Li, F., Jin, X., & Tang, Q. (2003). Recruitment, sustainable yield and possible ecological consequences of the sharp decline of the anchovy (Engraulis japonicus) stock in the Yellow Sea in the 1990s. *Fisheries Oceanography*, *12*(4–5), 495–501. https://doi.org/10.1046/j.1365-2419.2003.00262.x

Zhou, X., Sun, Y., Huang, W., Smol, J. P., Tang, Q., & Sun, L. (2015). The Pacific decadal oscillation and changes in anchovy populations in the Northwest Pacific. *Journal of Asian Earth Sciences*, *114*, 504–511. https://doi.org/10.1016/j.jseaes.2015.06.027